UCRL-16336

University of California

Ernest O. Lawrence Radiation Laboratory

HEAT TRANSFER CONSIDERATIONS IN DIFFERENTIAL CALORIMETER DESIGN

TWO-WEEK LOAN COPY

This is a Library Circulating Copy
which may be borrowed for two weeks.
For a personal retention copy, call
Tech. Info. Division, Ext. 5545

Berkeley, California

DISCLAIMER

This document was prepared as an account of work sponsored by the United States Government. While this document is believed to contain correct information, neither the United States Government nor any agency thereof, nor the Regents of the University of California, nor any of their employees, makes any warranty, express or implied, or assumes any legal responsibility for the accuracy, completeness, or usefulness of any information, apparatus, product, or process disclosed, or represents that its use would not infringe privately owned rights. Reference herein to any specific commercial product, process, or service by its trade name, trademark, manufacturer, or otherwise, does not necessarily constitute or imply its endorsement, recommendation, or favoring by the United States Government or any agency thereof, or the Regents of the University of California. The views and opinions of authors expressed herein do not necessarily state or reflect those of the United States Government or any agency thereof or the Regents of the University of California.

Research and Development

UCRL-16336

UNIVERSITY OF CALIFORNIA

Lawrence Radiation Laboratory
Berkeley, California

AEC Contract No. W-7405-eng-48

HEAT TRANSFER CONSIDERATIONS IN DIFFERENTIAL CALORIMETER DESIGN

Patrick Stephen Nicholson
(M. S. Thesis)

August 31, 1965

HEAT TRANSFER CONSIDERATIONS IN DIFFERENTIAL CALORIMETER DESIGN

Contents

Abstract v

I. Introduction 1

II. Development of the Differential Thermal Calorimeter . . 4

A. Differential Thermal Analysis and Refinements . . . 4

B. The Ideal Differential Thermal Calorimeter 9

III. Review of Previous Work in Differential Thermal Calorimetry 14

IV. Sources of Error in Previous Apparatus 21

V. Estimation of the Heat Content and Specific Heat of Silica (SiO_2) 23

A. Modification of Barner's Apparatus 23

B. Experimental and Results 24

VI. Cell Design and Heat Transfer Problems 29

A. Introduction 29

B. Theory 29

C. Procedure 31

D. Discussion of Results 33

VII. Use of Environmental Insulation Around the Differential Thermal Calorimeter Cells 38

A. Introduction 38

B. Procedure 38

C. Discussion of Results 40

VIII. Use of Powder as Environmental Insulation Around the Differential Thermal Calorimeter Cells 44

A. Introduction 44

B. Procedure 44

C. Discussion of Results 46

D. Conclusions 46

IX. Note on the Power Requirements of the Cells 51

X. Axial Heat Flow Between the Differential Thermal Calorimeter Cells 53

A. Introduction 53

B. Procedure 53

C. Discussion of Results 57

XI. Design of a Differential Thermal Calorimeter Capable of Producing Accurate Results 60

A. Design Principles 60

XII. Summary 65

Acknowledgments 67

References 68

HEAT TRANSFER CONSIDERATIONS IN DIFFERENTIAL CALORIMETER DESIGN

Patrick Stephen Nicholson

Inorganic Materials Research Division, Lawrence Radiation Laboratory,
and Department of Mineral Technology, College of Engineering,
University of California, Berkeley, California

August 31, 1965

ABSTRACT

Following early work on the development of a differential thermal calorimeter, an attempt has been made to eliminate the sources of error inherent in these designs.

Previous designs are discussed and criticized in detail, and a set of conditions postulated necessary for accurate work. Following these conditions, a series of modifications of apparatus design are reported. Heat transfer conditions in each system were investigated and are discussed. From these results, an ideal design is proposed which is based primarily on heat flow through packed powders.

I. INTRODUCTION

In the rapidly advancing field of ceramics, the need for fundamental knowledge of the basic properties of newly developed materials and of old long-established ones is imperative. The most important thermal properties to be considered in this connection are (a) heat contents and heat capacities, (b) heats of crystallographic transformation, and (c) heats of reaction.

Heat contents are usually measured by dropping a specimen of known weight and temperature into a mixture of ice and water. The decrease in the volume of the ice/water mixture due to melting can be related to the heat content of the dropped specimen. This technique is known as the "method of mixtures" or the dropping method. The reaction heat of solid/gas reactions is usually estimated using the bomb calorimeter. A mixture of the gas and the finely divided solid is exploded under pressure, and the heat involved obtained from the rise in temperature observed inside the bomb. The solution calorimeter is employed for estimating the heat involved in solid/liquid reactions. The isothermal and adiabatic calorimeters can be used for this purpose also.

The heat content of a substance is defined as

$$Q_p = (E_B - E_A) + P(V_B - V_A) , \qquad (1)$$

where Q_p is the heat absorbed at constant pressure in a change from state A to state B, V is the volume of the species, and E the internal energy.

Rearranging Eq. (1)

$$Q_p = (E_B + PV_B) - (E_A + PV_A) . \tag{2}$$

Defining a quantity H, the heat content, such that $H = E + PV$ and rewriting

$$Q_p = H_B - H_A = \Delta H . \tag{3}$$

Hence, the increase of heat content of a system is equal to the heat absorbed at constant pressure.

The definition of heat capacity (C) is

$$C = q/dT , \tag{4}$$

where q may be regarded as an infinitesimally small amount of heat absorbed by the system when the temperature is raised by dT degrees. When constant pressure conditions are employed, Eq. (4) may be restated

$$C_p = q_p/dT . \tag{5}$$

Since q_p, the heat absorbed, is equal to dH at constant pressure, it follows that

$$C_p = \left(\frac{\delta H}{\delta T}\right)_p$$

or

$$H_T = H_0 + \int_0^T C_p dT ,$$

where H_T is the heat content at T°K and H_0 is the internal energy at 0°K. For practical purposes this equation is usually written as

$$H_T = H_{298} + \int_{298}^{T} C_p dT . \qquad (6)$$

As ceramic articles are almost invariably fabricated from powders, this condition dictates the kinetics of all the reactions involved in their production. Hence, ceramic raw materials are difficult to analyze for thermodynamic properties because powders place severe limitations on the use of orthodox calorimeters.

Estimations of heat content by difference methods inherently involve large errors. Difference methods require high accuracies of measurement to obtain moderate accuracies in the resulting values.

This statement is particularly true for small differences between high measured values. A prime example is the heat of transformation of α-β quartz. In this case (H_{898} - H_{298}) for α-quartz is 8170 cal/mole and that for β-quartz is 8460 cal/mole. Thus, the transformation heat is 290 cal/mole.[9] A 1% inaccuracy in the measurement of H_α or H_β will produce a 28% error in the value of heat of transformation. Hence, such methods are highly unsatisfactory and more precise methods much preferred.

Another minor, yet sometimes important, drawback in the calorimeter methods is the time-consuming compilation of data.

From all these considerations it may therefore be considered that the ideal calorimeter for the accumulation of thermodynamic data for ceramics should (a) be operational up to high temperatures, (b) be capable of following continuously the slow evolution or adsorption of heat involved in both physical and chemical ceramic reactions, and (c) be able to compile data of high accuracy in a short time. The following sections discuss the development and design of such a calorimeter.

II. DEVELOPMENT OF THE DIFFERENTIAL THERMAL CALORIMETER

A. Differential Thermal Analysis and Refinements

It is well known that ceramic reactions are never instantaneous. Hence, the design of any calorimeter suitable for obtaining heat data of these reactions must necessarily be able to continuously follow the reaction in question and give an integral result. With the advent of highly sensitive electrical recorders, the technique of differential thermal analysis was developed for following such changes. The underlying principle of differential thermal analysis is to exploit the change in the thermal diffusivity of a substance while undergoing a physical or chemical reaction. When a species reacts, the rate of heat flow through it invariably changes. This change will be associated with a detectable temperature fluctuation. By comparing the temperature at the center of the reacting species with that of the center of an identical but inert species, the temperature change associated with the reaction itself can be recorded. On a differential temperature-vs-time plot, therefore, the reaction will appear as a differential-temperature peak. The size and direction of the peak and also the temperature at which it occurs are characteristic of the species under examination. This technique of comparing a temperature at a point in a reaction species with that of an identical point in an inert species is the principle of differential thermal analysis.

Basically, an apparatus for performing differential thermal analysis consists of three major parts: (a) a source of heat and its control, (b) a test block, and (c) method of recording heat effects. The usual

source of heat is a tubular furnace with a current input capable of maintaining the desired heating rate. The test block most often consists of a rectangular parallelepiped of metal with two holes opening at the top, one for the sample and one for the reference material. This block is so constructed as to facilitate correct positioning of the differential thermocouple and the thermocouple registering the test block temperature.[1] The environmental furnace is raised in temperature at a constant rate. The differential temperature and block temperature are monitored. Endothermic and exothermic reactions evidence themselves as peaks on the differential temperature plot. The exact temperature at which these reactions take place can be inferred directly from the metal-block temperature reading.

The height and width of the peaks obtained indicate the kinetics of the reactions taking place. While being an excellent tool for qualitative identification of mineral constituents and other qualitative work, the quantitative application of the technique is questionable. Some investigators have considered the area under the endothermic and exothermic peaks to be a measure of the heat involved in these reactions. Attempts have been made to calibrate the apparatus using reactions of known heat characteristics,[2,3] but errors inherent in the technique must render these results unsound.

Boersma[4] made a mathematical analysis of the heat flow involved in differential thermal analysis and derived equations for the calculation of peak areas for a sample in the form of a cylinder, sphere, or flat plate. However, he realized that his assumption that the thermal

conductivity of the sample and the inert material are the same and remain at the same level during a transition was in error. This assumption is not valid if the transition involves a gas.

In differential thermal analysis the temperature-sensing device rests in the middle of the powder sample. It consequently indicates heat changes in its immediate surroundings and also heat conducted to it through the sample from non-neighboring regions. It will be demonstrated later that the thermal conductivity through a packed powder is primarily due to the gaseous phase within it. As pores are very small, the only mode of heat transfer in the gas must be conduction.

The thermal conductivities of dilute monatomic gases are well understood and can be predicted by the kinetic theory. For polyatomic gases, the theory is not fully developed but some useful approximations can be made.

It can be shown[5] that the thermal conductivity of a monatomic gas k is

$$k = \frac{1}{d^2}\sqrt{\frac{K^3T}{\pi^3 m}} , \tag{7}$$

where K is the Boltzmann constant, d is the diameter of molecule, and m is the mass of molecule.

For a polyatomic gas, Euchin[6] showed that

$$k = (C_p + \frac{5}{4}\frac{R}{M})\,\mu , \tag{8}$$

where μ is the coefficient of viscosity of the gas, M is the molecular weight, and R the gas constant.

Both relations show that

$$k \propto 1/M . \tag{9}$$

Hence, the thermal conductivity of gases of high molecular weight is lower than those of low molecular weight. In Table I are listed values of thermal conductivity for some common gases. The theoretical relationship is seen to hold in practice. Many of the reactions investigated in the field of ceramics by differential thermal analysis involve the evolution of a gas. It is observed that reactions involving CO_2 give more marked peaks than those involving H_2O. This is not entirely due to the quantity of heat involved in the reaction but must also depend on the thermal conductivities of the two gases. This fact, therefore, constitutes a grave error in any quantitative results obtained by differential thermal analysis even if a careful calibration is carried out. (It should be noted that a calibration involving the same gaseous product as expected in the differential thermal analysis of given sample could well be used to give quantitative results for that sample.) For this reason, a method of measuring heat independent of temperature effects but based on heat flow will ensure more accuracy. One possible method is to measure the actual differential heat supplied to an unknown material vs an inert standard under dynamic conditions. This is the basis of differential calorimetry. A small heater is incorporated in the inert and sample cells. Constant power is maintained to the sample and a variable power to the inert reference. This will provide a means of eliminating any differential temperature generated due to physical or chemical reactions in the sample.

Table I. Thermal conductivity of some gases.

Gas	Molecular weight	Thermal conductivity (cal/°C/mole/sec)
Helium	4	339×10^{-6}
Methane	16	64×10^{-6}
Nitrogen	28	52×10^{-6}
Carbon monoxide	30	49×10^{-6}
Argon	40	38×10^{-6}
Carbon dioxide	46	30×10^{-6}

In differential thermal analysis, the size and shape of a differential temperature peak are dictated by the reaction heat involved and the thermal diffusivity of the sample. However, in differential thermal calorimetry the rate of heat flow away from the two cells containing the sample and the inert standard to their environment is independent of the sample diffusivity. Consequently, the applied power is a direct measure of the reaction heat alone. This technique, therefore, eliminates the main source of error which renders differential thermal analysis unsuitable for quantitative work.

B. The Ideal Differential Thermal Calorimeter

The basic principle of the differential thermal calorimeter is to supply or abstract heat to or from a reacting system so as to maintain the temperature at some point in the system, the same as that of a similar point in a physically identical inert system. This is done by using two identical cylindrical metal cells, each with a small cylindrical heater down its center. The sample and the inert substance are packed one into each cell between the heater wall and the outer cell wall. End-caps are used to complete the containers. The two beads of a differential thermocouple are located at identical positions on the outer wall of each cell, and the differential temperature of these two positions maintained at zero by supplying power to the cell heaters as required. The necessary power to maintain this status quo is plotted on a time base, and a direct measure of any heat effects in the sample thus obtained.

Considering therefore the mechanism by which the differential thermal calorimeter system gives results, a number of points can be drawn up essential for its functioning correctly:

(a) Each cell must be identical and be subject to identical environmental conditions.

(b) All the heat supplied to the sample must come from the cell heater, i.e., heat must always flow out of the cell.

(c) The response of the inert cell must be as quick as possible so as to maintain adequate control of the system.

(d) The gradient across the sample must be as small and as constant as possible.

(e) All heat must flow radially from the cell, i.e., through the powder.

(f) The cells must be completely thermally isolated from each other.

Taking each point in turn, the symmetry of the system, consistent with constructional considerations, can be assured as far as possible. With regard to point (b), it might be assumed that if the cell center is hotter than the cell wall, heat must be flowing from the cell at all times. However, there are circumstances when this is not true. The specimen powder is subject to two sources of heat, the cell heater and the main furnace. It is essential for the differential operation that all heat from the cell heater should flow outward through the cell contents to the differential thermocouple. Consider five hypothetical

temperatures, T_1 to T_5, across a section of the furnace corresponding to the center of the filled cell (Fig. 1). For all the heat from the cell heater to flow outward through the sample,

$$T_1 > T_2 > T_3 > T_4.$$

It might be assumed that for these conditions it is enough that $T_1 > T_3$. This is a fallacy. If $T_3 < T_4$ then even though $T_1 > T_3$, a gradient can develop such that $T_2 < T_3$ (see b in Fig. 1). Hence, the temperature minimum will be within the sample instead of being at the cell wall or beyond. This means that any heat pertaining to the powder sample conditions (the prime effect being measured) will not travel to the cell outer wall but to the new minimum point. Such a situation would lead to erroneous results.

The response of the inert or active cell to any change in a sample cell must be immediate. The sensitivity of the response, therefore, depends entirely on the thermal conductivity of the inert species in the cell. This conductivity should be as high as possible and thus an empty cell might be used.

The fourth point is concerned with an error due to the sample width. The actual temperature of the sample is measured at the outside cell wall and this temperature, therefore, will be a little below the average sample temperature. However, as long as the gradient across the cell is small, this error is not too large. The larger this gradient, the larger the error and to minimize this the powder thermal conductivity should be as large as possible.

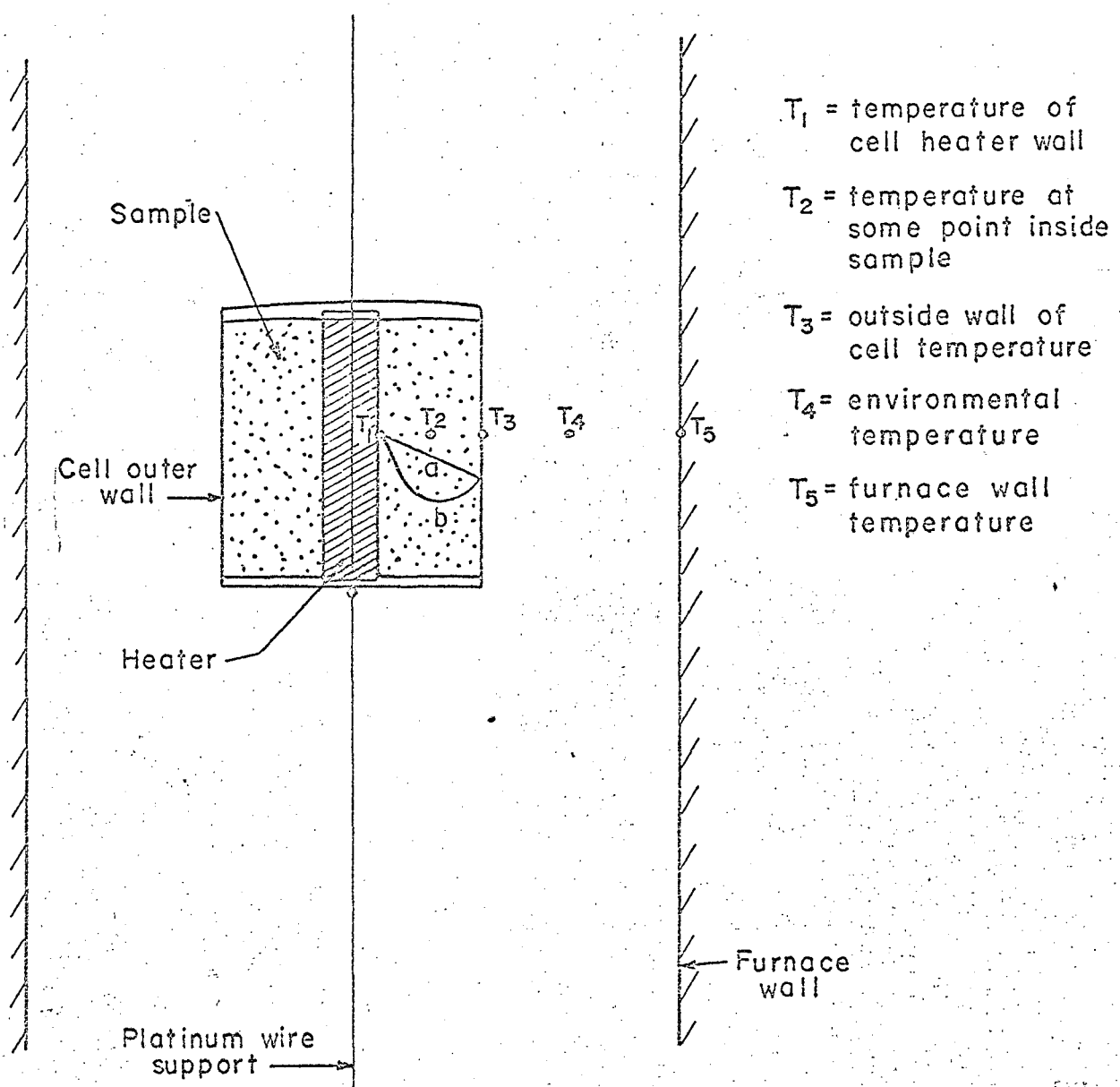

FIG. I DIAGRAMMATICAL REPRESENTATION OF A DIFFERENTIAL CALORIMETER CELL AND ITS ENVIRONMENT.

Considering point (e), the power applied to the cell heater must all be transferred to the sample or erroneous values will result. For this reason, the heat flowing axially from the cells must be kept to a minimum. In the same way, any thermal link between the sample cell and the inert reference cell must be assiduously avoided since exchange of energy between the two will introduce errors.

III. REVIEW OF PREVIOUS WORK IN DIFFERENTIAL THERMAL CALORIMETRY

The first apparatus to utilize the differential power concept was that of Clareborough and coworkers.[7] They measured the increase in internal energy produced in a metal during plastic deformation. Cylindrical specimens, one deformed and one annealed, were placed side by side but not in contact inside an isothermal enclosure under vacuum. Each specimen was heated inside by a small heating element. During heating the temperatures of the two specimens and the enclosure were maintained the same. The stored energy was measured as the difference in the amounts of electrical energy required to heat the specimens through the temperature range in which the energy stored during deformation was released. A differential wattmeter was used to measure the difference in the power supplied to the specimens. The stored energy was obtained by integration of the power difference-vs-time curve.

The design of the apparatus was such that the two specimens of metal were supported by a tubular metal boss and linked by this same boss. The heat effect being measured was by nature very small. The offering of alternative paths for heat dissipation in the form of supports and interlinks must necessarily make the measured value even smaller. It is essential that the differential couple should receive a true sample of the temperature produced by <u>all</u> of the heat effect, i.e., all alternative flow paths from the specimen should be eliminated.

One striking advantage of metal specimens over ceramic ones is the marked difference in thermal conductivity. Sensitive control of the system requires good specimen conductivity. To maintain the differential

temperature at zero all the time, it is essential that any heat change should be instantly transmitted to the temperature-recording power control device. This will allow the applied compensating power to keep directly in step with the heat change. In the design of a differential thermal calorimeter applicable to ceramic materials in the form of powders, this constitutes one of the major problems.

The first attempt in this field was made by J. O. Barner.[8] As the main work described in this present dissertation is concerned with the improvement of Barner's design, his work will be reviewed in detail. As previously mentioned, most ceramic raw materials are powders; hence, retaining vessels or cells must first be designed to contain a powdered sample and the inert reference material. The low thermal diffusivity of the ceramic powder makes it essential, for reasons of control, to limit the sample dimensions between the heat source and the temperature-sensing device. The heat flowing to the thermocouple bead must also be representative of the heat effects involved in the powder. Hence, the differential thermocouple should lie in the direction of primary heat flow. Barner's apparatus is shown in Fig. 2. The cells consisted of metallic concentric tubes, 1a and 1b, and the powder sample filled the annulus between the tubes of the top cell (1a). The inner tube contained the heater and the outer tube was the cell wall. The tubes and the cell lids were fabricated from platinum. On the outside wall of each cell platinum buckets were affixed to contain the differential (6a) and monitoring (6b) thermocouples. To minimize radiation heat transfer between the cells, they were mounted vertically on a central tube (3).

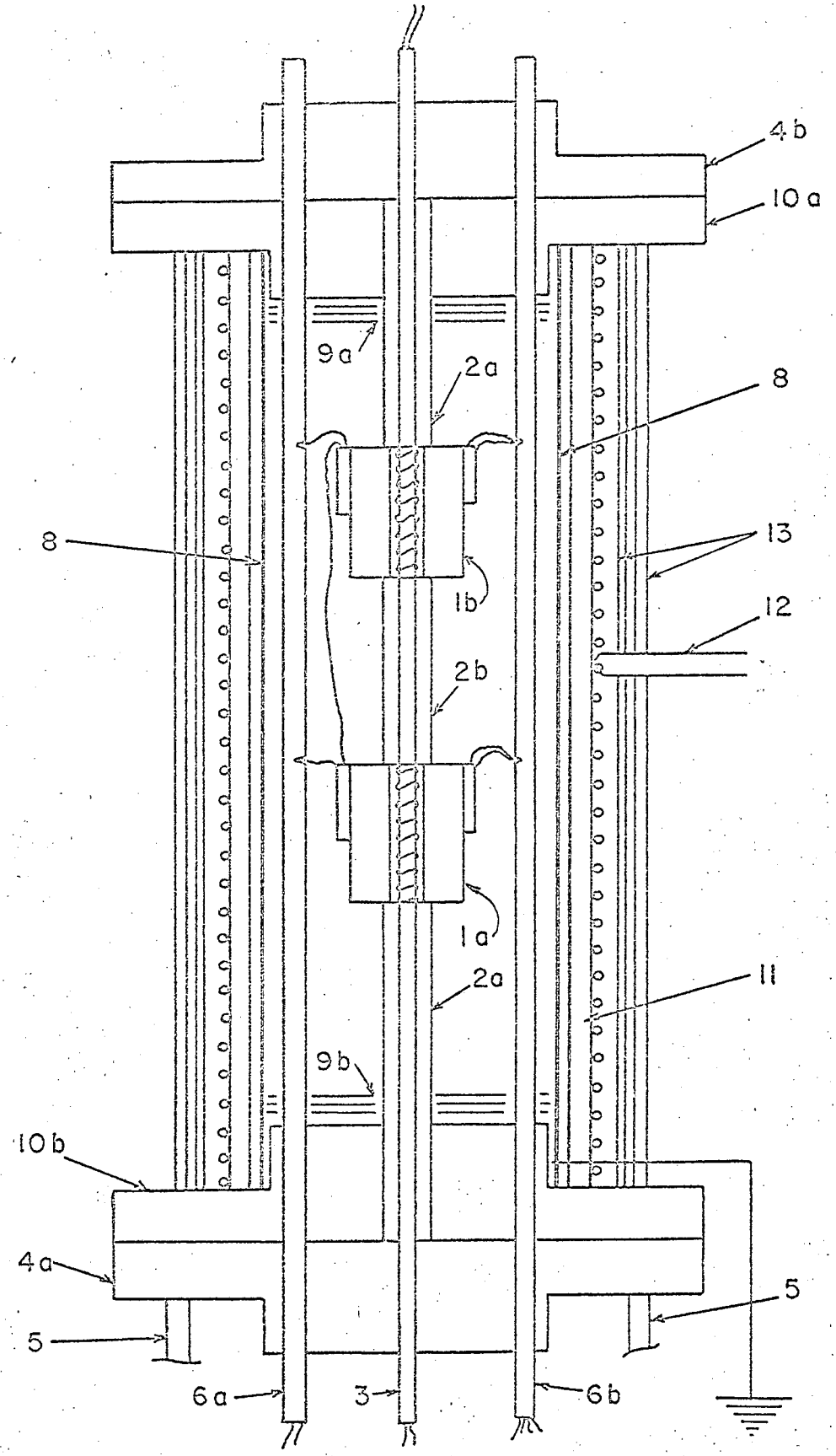

FIG. 2 FURNACE ASSEMBLY OF BARNER.

The circuits used by Barner to link up the various operations in the control sequence are shown in detail in his thesis.

To increase the sensitivity of the power-active cell, it was found necessary to leave it empty of the inert material. In this way the heat lag due to the thermal diffusivity of the inert powder was eliminated. Having filled the top cell with the sample of known weight, both cells were introduced into the furnace. This was then flushed thoroughly with helium and all the monitoring circuits allowed to equilibrate. The environmental furnace temperature was then raised at a controlled rate to a new temperature and allowed to soak. During the temperature rise the power to the empty cell was seen to lag behind that of the full cell owing to the heat capacity of the powder sample. The differential power curve, therefore, reached a dynamic equilibrium at a level below that of the static soak conditions. Any physical or chemical reaction during the period of temperature rise was superimposed on the heat capacity curve. The whole picture can best be seen by referring to Fig. 3.

At time T_1 the furnace temperature started to rise. Owing to the heat capacity of the sample, the empty cell gained in temperature. To keep the cell differential temperature at zero, the power to the empty cell was cut back. This shows in the differential power curve, ΔP. When dynamic equilibrium had been established, the full cell lagged by a constant amount and the power curve reached a constant level. At time T_2 an endothermic reaction took place in the sample necessitating a further step back of the power to the empty reference cell. The reaction

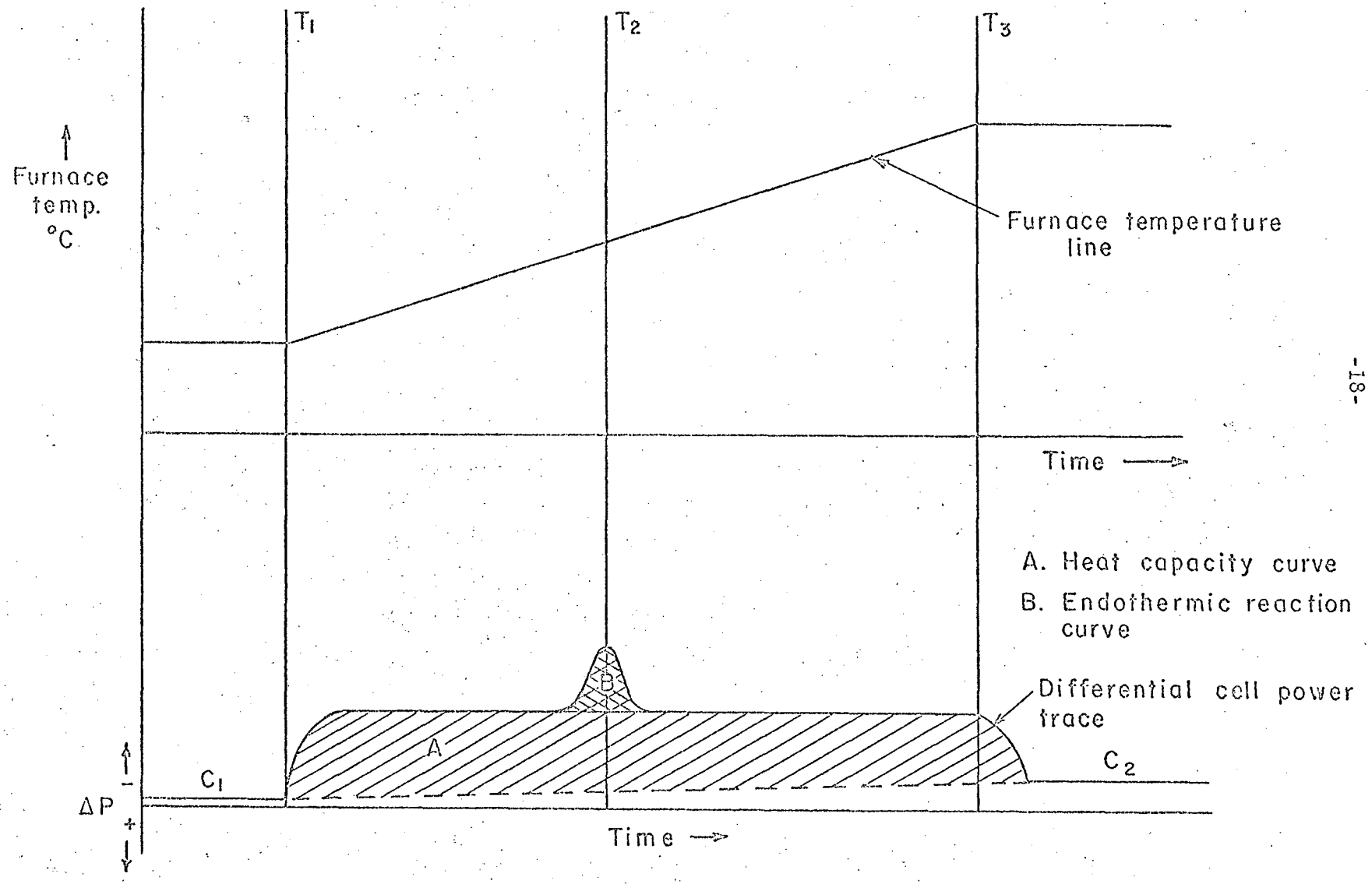

FIG. 3 FURNACE TEMPERATURE AND CORRESPONDING DIFFERENTIAL POWER CURVES.

complete, the power returned to the original dynamic equilibrium level. The curve dropped to level C_2 with the advent of the new soak period.

Integration by polar planimeter of the crosshatched area yielded the heat absorbed in the unknown material between the two temperatures involved. The heat involved in the endothermic reaction can be estimated in the same way. Using this technique, Barner measured the heats of crystallographic transformation of quartz, potassium sulfate, and iron sulfide. He also measured the heat contents of silica and a mixture of potassium sulfate and alumina. His results are tabulated in Table II together with the accepted values[9] and the accompanying errors.

Table II. Results obtained by Barner.

Heats of transformation			
Material	Measured H_T cal/mole	Published H_T cal/mole	% Difference
SiO_2	198	290	-31.9
K_2SO_4	2309	2140	+ 7.9
FeS	154	120	+29.2

Heat contents			
Material	Measured Heat content	Published Heat content	% Difference
SiO_2	3140	2255	+39.2
$K_2SO_4 + Al_2O_3$	2070	1722	+20.2

IV. SOURCES OF ERROR IN PREVIOUS APPARATUS

For any heat measurement by this technique to be meaningful, it is essential that both cells be physically identical. This identity pertains to the cell components and to their physical environment. The apparatus used by Barner did not satisfy the second of these conditions. The heat flow inside the environmental furnace cannot have been uniform as the furnace design was unsymmetrical. The top of the furnace casing was water-cooled, whereas the base was not. The bottom of the casing was in direct thermal contact with a heavy iron stand. All the wires used to transmit the various thermocouple signals from inside the furnace were brought out of the bottom of the apparatus further upsetting the symmetry.

Consequently, it is quite possible that a temperature gradient existed down the length of the furnace core. This gradient alone would be enough to produce non-identical conditions around each cell, but in a gaseous atmosphere the situation will be further compounded. The convection currents produced in the gas by such gradients will further reduce conditions of identity between the cells.

The second cardinal necessity for the acquisition of reliable results is that the cells should be thermally isolated from each other. The two-cell heaters in Barner's equipment were wound on the same alumina tube (see 3 in Fig. 2). The two cells were further interconnected by an alumina tube of larger bore that fitted around the heater tube (see 2a, 2b, and 2c in Fig. 2). These alumina tubes constituted a direct thermal link between the two cells; hence, any difference in temperature between the two due to the sample reaction would induce intercell heat flow and therefore lead to errors.

Consider now the design of the cells themselves. It has already been noted that the primary path of heat flow must be from the cell heater, through the sample, to the thermocouple on the outer wall. However, the use of platinum end-caps for the cells offers an alternative and much easier thermal path between the heater and the cell wall. Any heat transfer taking place by this route will evade the powder sample and give rise to further errors. The platinum cell ends also constitute an electrical conduction path between the heater and the differential thermocouple. At high temperatures, stray electrical signals filtering from the now-conducting alumina tubes to the thermocouple will cause differential temperature signal errors.

This accumulation of discrepancies will give rise to large errors. At the beginning of the present work, an attempt was made to eliminate them. A further source of error involving temperature gradients was, however, brought to light but, although relevant to Barner's system, it will be discussed at a later stage.

V. ESTIMATION OF THE HEAT CONTENT AND SPECIFIC HEAT OF SILICA (SiO_2)

A. Modification of Barner's Apparatus

Considering the sources of error inherent in Barner's design, the whole furnace and cell complex was redesigned. The main structure was made completely symmetrical. An equal number of exit ports were located in the top and lower portions of the main furnace case. These facilitated the passing, via glass-metal vacuum seals, of the heater and thermocouple leads associated with the cells and the environmental furnace. The form of the furnace coil was changed. However, this modification was not permanent and was further varied in subsequent designs. The core was wound of A-1 Kanthal wire on an alumina core. To eliminate environmental temperature gradients in the furnace, a heavy nickel tube was placed inside it and this constituted the radiating surface area seen by the cells. This tube was grounded outside the furnace so eliminating any induction effects due to the heating coil. To preclude axial heat losses from the furnace, the nickel tube was not carried to the ends of the furnace proper. It was maintained in the center by an alumina collar at either end. The whole assembly was supported on a steel plate resting on lugs welded to the inside of the outer case. The void between the furnace core and the water-cooled outer case was filled with bubbled alumina insulation.

The configuration of the cells was unchanged; however, the alumina tubing support was replaced by a platinum wire and the platinum cell end-caps were replaced by boron nitride ones. The cells were spaced by porcelain insulation beads. Two nickel sheet baffles were placed half

way down the bead row, lying exactly between the cells and in the center of the furnace. These served to eliminate any convection currents between the cells and also between their immediate environments.

The cell heaters were wound on boron nitride formers and platinum foil replaced the platinum buckets for the attachment of the thermocouples. Boron nitride has a high electrical resistivity and facile machinability. It also has a lower thermal conductivity than platinum and, therefore, decreases the heat flow around the powder through the cell material when used for the cell caps. The modified design of the cells is shown in Fig. 4. The use of platinum foil ensured thermal contact between the differential bead and the cell wall. The thermocouple bead was simply pinched into the foil. The cell temperature was monitored on the outside wall by a standard Pt/Pt 10% Rh thermocouple with the bead recessed into the porcelain shielding. This precaution was necessary, for electrical contact between the monitor and differential thermocouples must be assiduously avoided or cross-talk between their respective recorders will lead to errors. The error in the temperature reading due to the recession of the bead is very small, for the bead is completely surrounded by the connecting foil.

B. Experimental and Results

A sample of -200 ground quartz was carefully packed into the top cell and its weight ascertained by difference. Both cells were then assembled on the supporting wire and all the electrical and thermocouple circuits tested for continuity. Electrical contact between the differential couple and the cell walls was checked. The whole assembly was

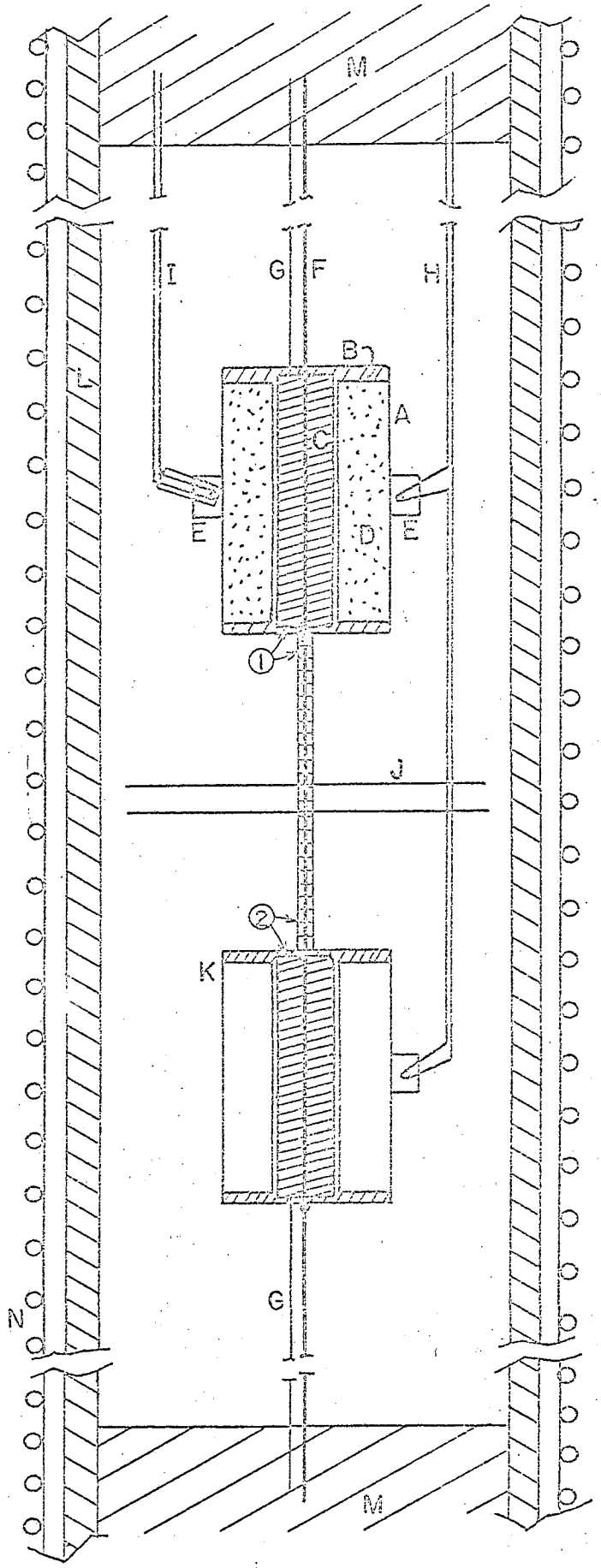

A. Sample cell
B. Boron Nitride ends
C. 5 Ω resistance heater of Pt wire wound on Boron Nitride
D. Sample powder
E. Pt foil to be wrapped around thermocouple beads
F. Pt support wire. Also acts as a common leg to both heaters through ① and ②
G. Other leg of heater
H. Differential thermocouple
I. Monitor thermocouple
J. Nickel baffles
K. Empty cell
L. Grounded Nickel tube
M. Insulating end plugs
N. Kanthal A-1 furnace coil on Al_2O_3 former

FIG. 4 CELL ASSEMBLY.
MODIFICATION I.

maintained in the center of the furnace by passing the support wire up through a hole in the top insulating plug and fixing it with a collar. The thermocouples and electrical leads emerged from other holes in the same plug. The bottom plug was affixed when the cells were in position in the furnace. Similar holes in it also served to transport electrical leads. The center support wire was used as a common leg for both cells, one end of each heater being wrapped around it. The other two heater ends were brought directly out the top and bottom plugs, respectively, and the cell-heater circuits completed. The control circuits were the same as those used by Barner. However, the power signals from each cell were fed directly into a two-point recorder and not differentially into a single-pen instrument. Hence, a base power trace was obtained. This enabled the estimation of the power-plot drift due to the increase of the cell-heater resistance with increasing temperature and therefore ensured measurement of the correct area under the power-vs-time plot. Having assembled the cell complex inside the furnace and inserted the bottom end-plug, the top and bottom of the water-cooled furnace were placed in position and the whole assembly pumped down to a vacuum of approximately 10^{-3} torr. After pumping for half an hour, the whole tank was flushed with helium for 5 min and then the flow damped down to 2 to 3 cc/sec. An equal power of 5 W was fed to each cell heater and an equilibrium heat flow allowed to establish. The environmental furnace was then raised in temperature at a rate of 140° C/hr for half an hour and then allowed to soak at the temperature attained for a further half hour. This cycle was then repeated until a temperature of 660° C had been reached. During this time the differential temperature

between the cells was controlled to ±0.002 mV (±0.5°C) and the sample cell temperature and both cell-heater powers carefully monitored.

The difference in power consumption between the cells for given temperature intervals was then estimated by measuring the area under the variable power curve with a polar-planimeter. The base line slope was obtained from the constant power cell plot.

The results of several estimations of this sort were averaged and are shown plotted in Fig. 5. Also plotted are the accepted values for silica in the same temperature range.[9] The average error ranges from -11% to -27%.

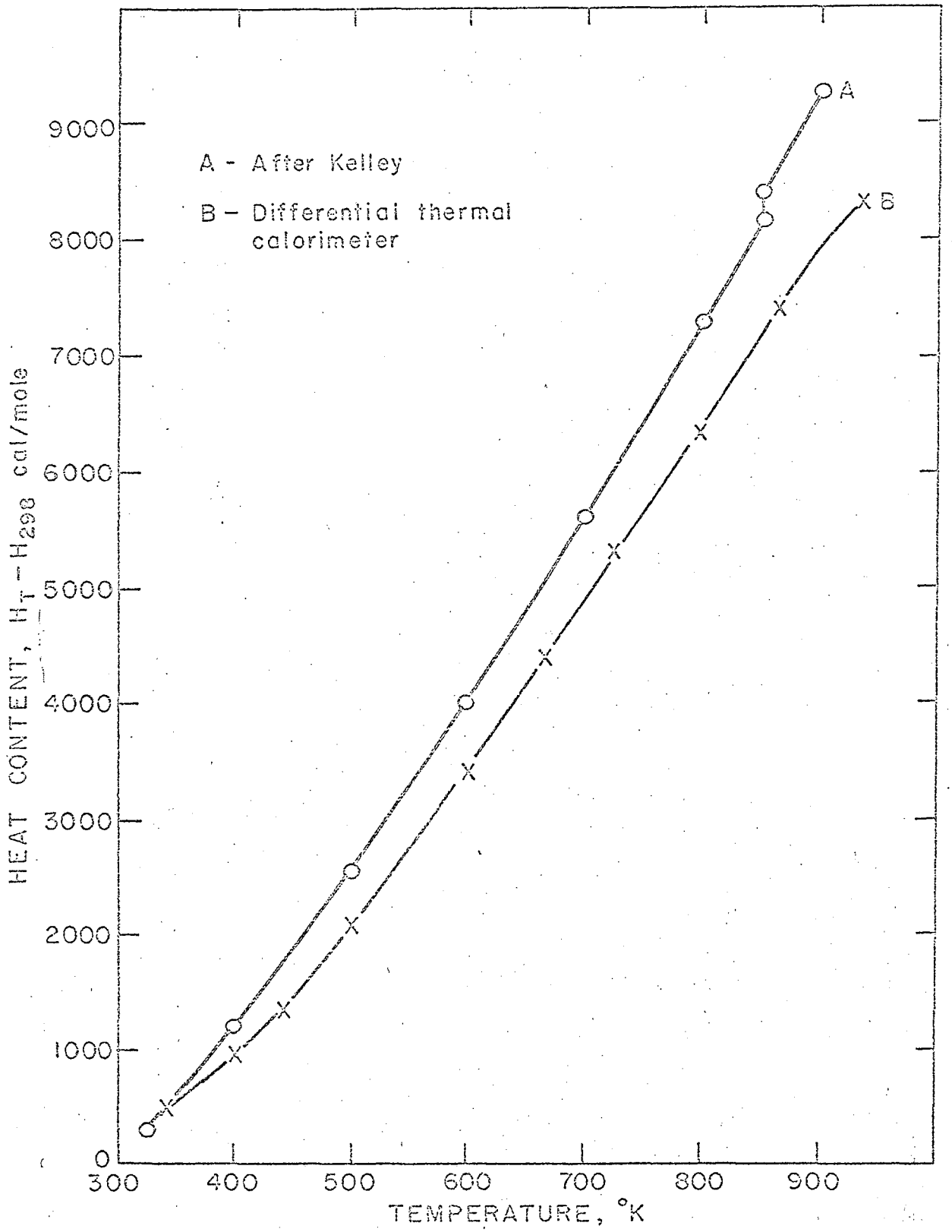

FIG. 5 HEAT CONTENT vs. TEMPERATURE FOR SILICA.

VI. CELL DESIGN AND HEAT TRANSFER PROBLEMS

A. Introduction

Although the average error in the estimation of the heat content of silica reported in the last section is much less than that reported by Barner (39.2%), it is evident that the system is far from perfect.

In the introductory discussion, ideal heat transfer conditions necessary for accurate results were postulated. The maintenance of these conditions depends on the thermal characteristics of the cell system. For this reason an investigation of the system heat transfer conditions was undertaken with a view to designing a thermally ideal cell. During the first part of the furnace cycle, the temperature of the whole system is increasing. Heat transfer conditions during this period would be extremely hard to analyze, so those of the steady-state or soak period were investigated. By making a continuous plot of the relevant temperature gradients, however, the correct temperature sequence could be maintained throughout the whole cycle. A study of this nature will produce values of the "effective" thermal conductivities of the various parts of the system. This knowledge will facilitate proper cell design.

B. Theory

The cell system can be divided into two parts, i.e., the cell itself and its environment. As a powder is present in the cell, the gaseous phase in the full cell exists in continuous pores of very small dimensions. Heat transfer by convection can, therefore, be neglected. Assuming radial heat flow only and neglecting end-effects, the cell can

be regarded as a cylindrical tube of infinite length with the tube wall made of a gas-powder composite. This assumption is not strictly correct, but the boron nitride ends of the cell render it a good approximation.

The standard heat transfer equation for steady-state conditions is

$$q_k = -kA \frac{dT}{dr} , \tag{10}$$

where q_k is the rate of heat flow by conduction, k is the thermal conductivity, A is the conducting area, T is temperature, and r is the thickness of conductor.

For a cylinder $A = 2\pi r\ell$, where ℓ is length of cylinder; hence,

$$q_k \int \frac{dr}{2\pi r\ell} = -k \int dT . \tag{11}$$

For a circular pipe of inner radius r_i and outer radius r_o, Eq. (11) gives

$$\frac{q_k}{2\pi\ell} \ln \frac{r_o}{r_i} = k(T_i - T_o) \tag{12}$$

or

$$k = \frac{q_k \ln r_o/r_i}{2\pi\ell \, \Delta T} . \tag{13}$$

The environment around the cell is gaseous so all three modes of heat transfer are now relevant. Lumping the conduction and convection coefficients together as h_c and using h_r for the radiation coefficient, the total heat transfer coefficient may be written $(h_c + h_r)$.[10]

Taking a characteristic dimension of the heat transfer surface, i.e., the area A_s, the rate of heat transfer is given by

$$q = h_c A_s (t_s - t_a) + h_r A_s (t_s - t_e), \tag{14}$$

where t_s is the temperature of the body surface, t_a is the gas temperature, t_e is the temperature of enclosing walls, and q is the rate of heat flow. Assuming that the gas is at approximately the temperature of the furnace wall in contact with it, $t_a = t_e$ and consequently

$$(h_c + h_r) = \frac{q}{A_s (t_s - t_a)}$$

or

$$(h_c + h_r) = \frac{q}{2\pi r \ell (t_s - t_a)} . \tag{15}$$

C. Procedure

A small hole was drilled in the cap of the top cell and a thermocouple introduced to measure the heater wall temperature. Two other thermocouples were set up, one on the outer wall of the cell and one 1/4 in. away in the environment. All three signals were printed out on a multipoint recorder. Hence, four temperatures were monitored as shown in Fig. 6.

The sample cell was filled with A-14 alumina powder and the initial procedure followed as before. Helium was used as the inert gaseous phase. The temperature was increased at the rate of 180°C/hr for half an hour and then the system was allowed to equilibrate for the same period of time. At the end of this period the four temperatures (T_1, T_2, T_3, and T_4) were read. The temperature was then increased to 800°C following this one-hour cycle. Throughout the entire experiment, the power to the cells was adjusted when the gradient conditions required it.

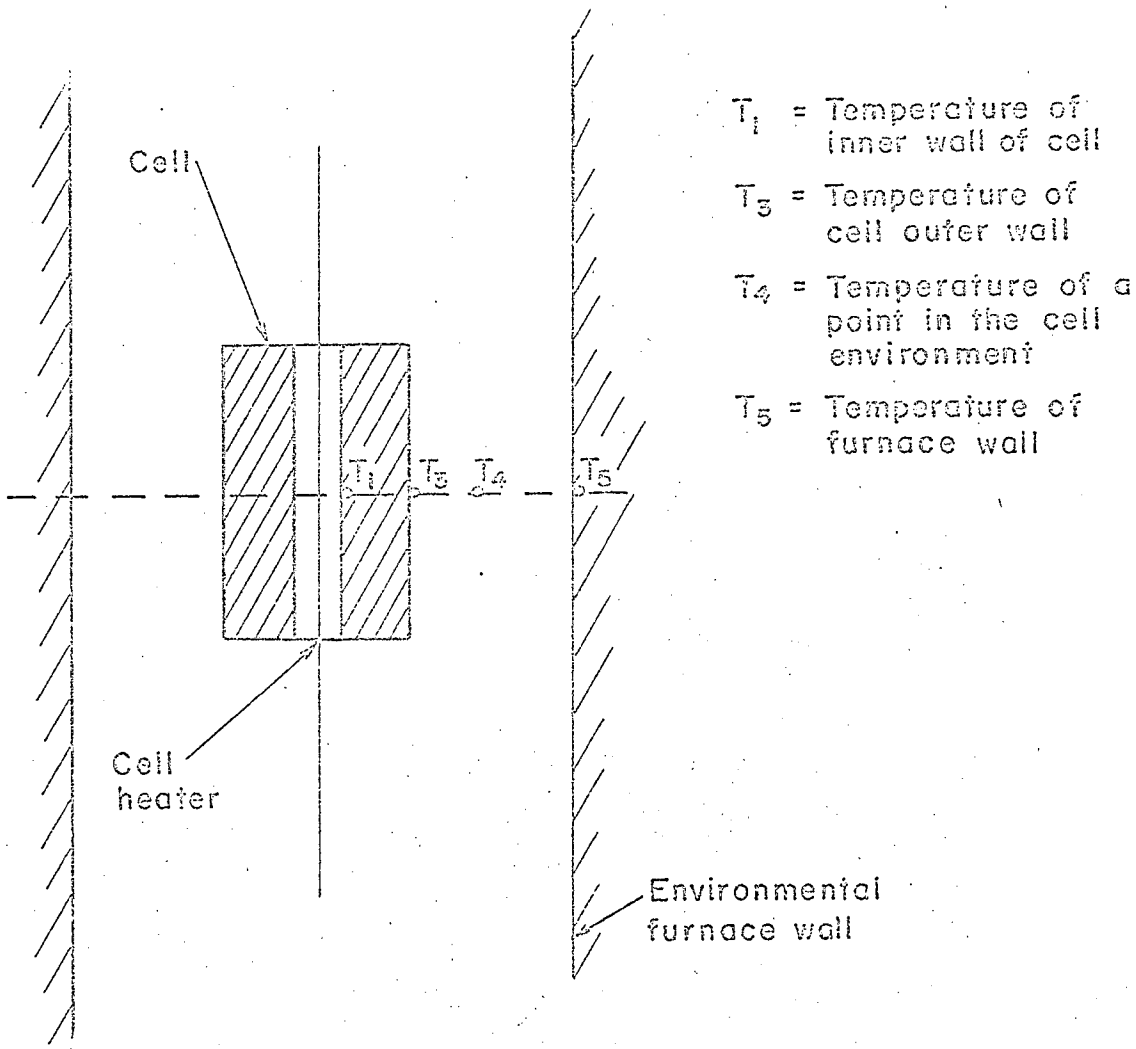

$\Delta T_1 = T_1 - T_3$ = Temperature gradient across the cell.

$\Delta T_2 = T_3 - T_4$ = Temperature gradient from the cell outer wall to a point in the cell environment.

$\Delta T_3 = T_4 - T_5$ = Temperature gradient between the cell environment and the furnace wall.

FIG. 6 POSITIONS OF THERMOCOUPLES IN HEAT TRANSFER INVESTIGATION OF 1st MODIFICATION OF BARNERS APPARATUS.

In this way the temperature sequence $T_1 > T_2 > T_3 > T_4$ was carefully maintained. Identical runs were performed in argon and vacuum.

Plots were made of the temperature gradients across the system vs the furnace temperature and these are shown in Figs. 7, 8, and 9.

D. Discussion of Results

If all the heat required by the sample is to be supplied by the cell heater, it is essential that $T_3 > T_4$. It is also desirable to maintain a steady gradient across the sample with temperature so that dynamic equilibrium conditions may apply. The sample gradient should also be as small as can be acquired consistent with $T_3 > T_4$. Hence, an ideal ΔT-vs-T plot would be three horizontal parallel straight lines in the positive quadrant. Considering the three plots made, a helium atmosphere gives the lowest temperature gradient across the sample and the least change of this gradient with temperature; however, argon best maintains the $T_3 > T_4$ condition. The gradient across the sample under vacuum conditions is so high as to make accurate assessment of the mean sample temperature impossible and, therefore, no further vacuum work was undertaken.

The system response was best in helium and this atmosphere facilitated sensitive control. The argon system was less sensitive and virtually no control was possible in vacuum. These observations are consistent with the sample "effective" conductivity values obtained in each case, i.e.,

(K_1) in helium, 18×10^{-4} cal/sec/°C/cm (40°C)

to 40×10^{-4} cal/sec/°C/cm (750°C)

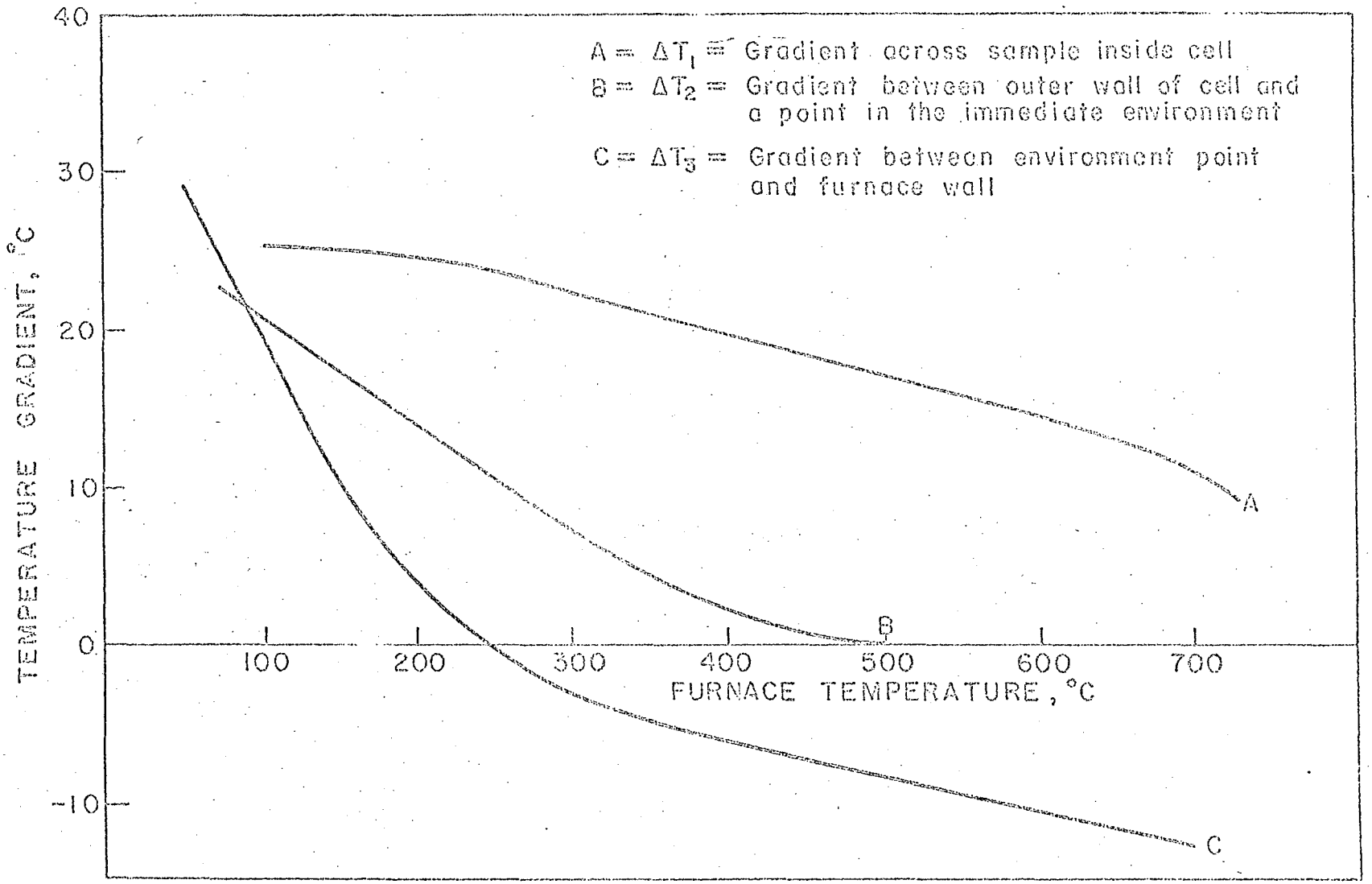

FIG. 7 PLOT OF TEMPERATURE GRADIENT vs. ENVIRONMENTAL FURNACE TEMPERATURE. HELIUM ATMOSPHERE.

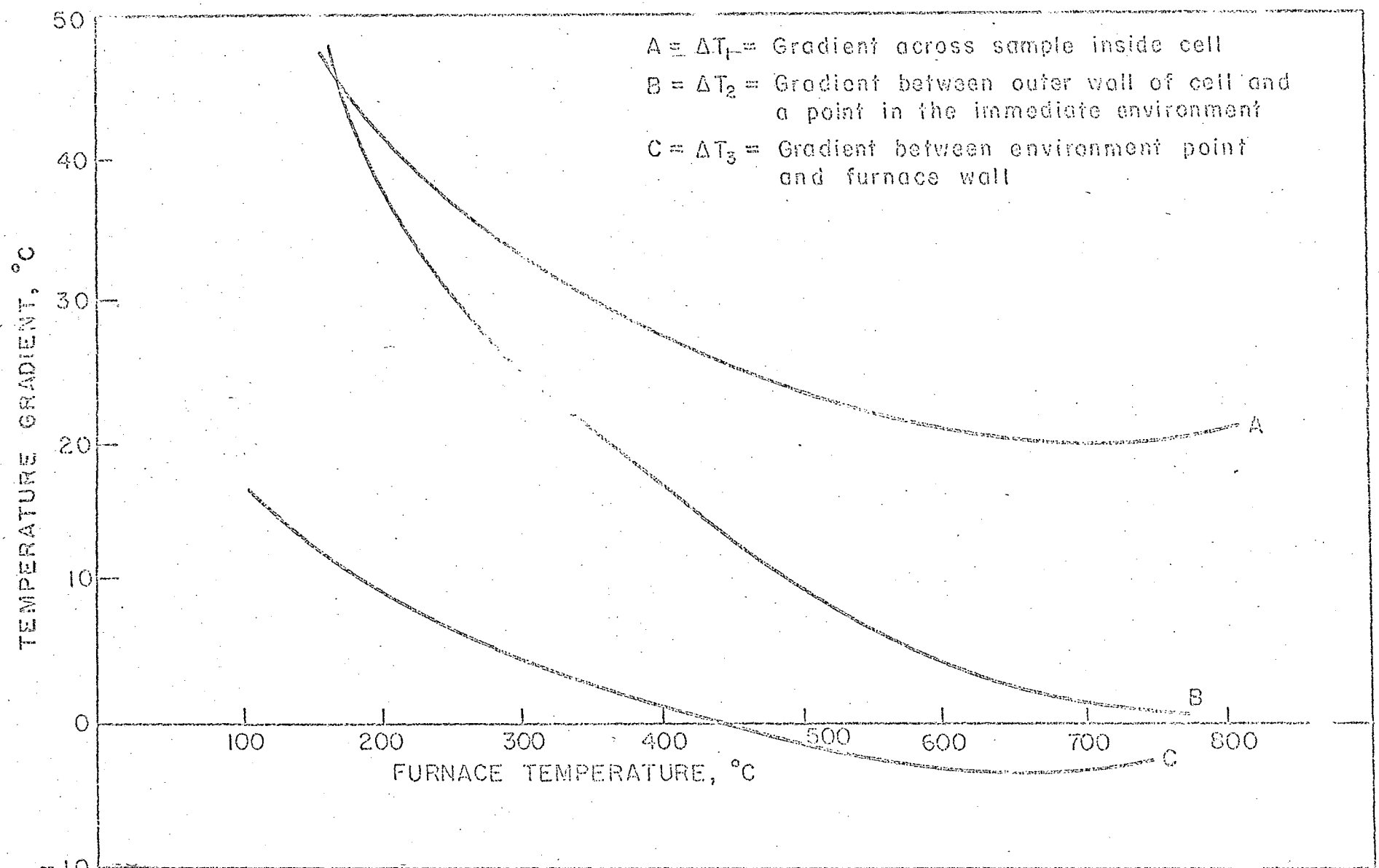

FIG. 8 PLOT OF TEMPERATURE GRADIENT vs. ENVIRONMENTAL FURNACE TEMPERATURE. ARGON ATMOSPHERE.

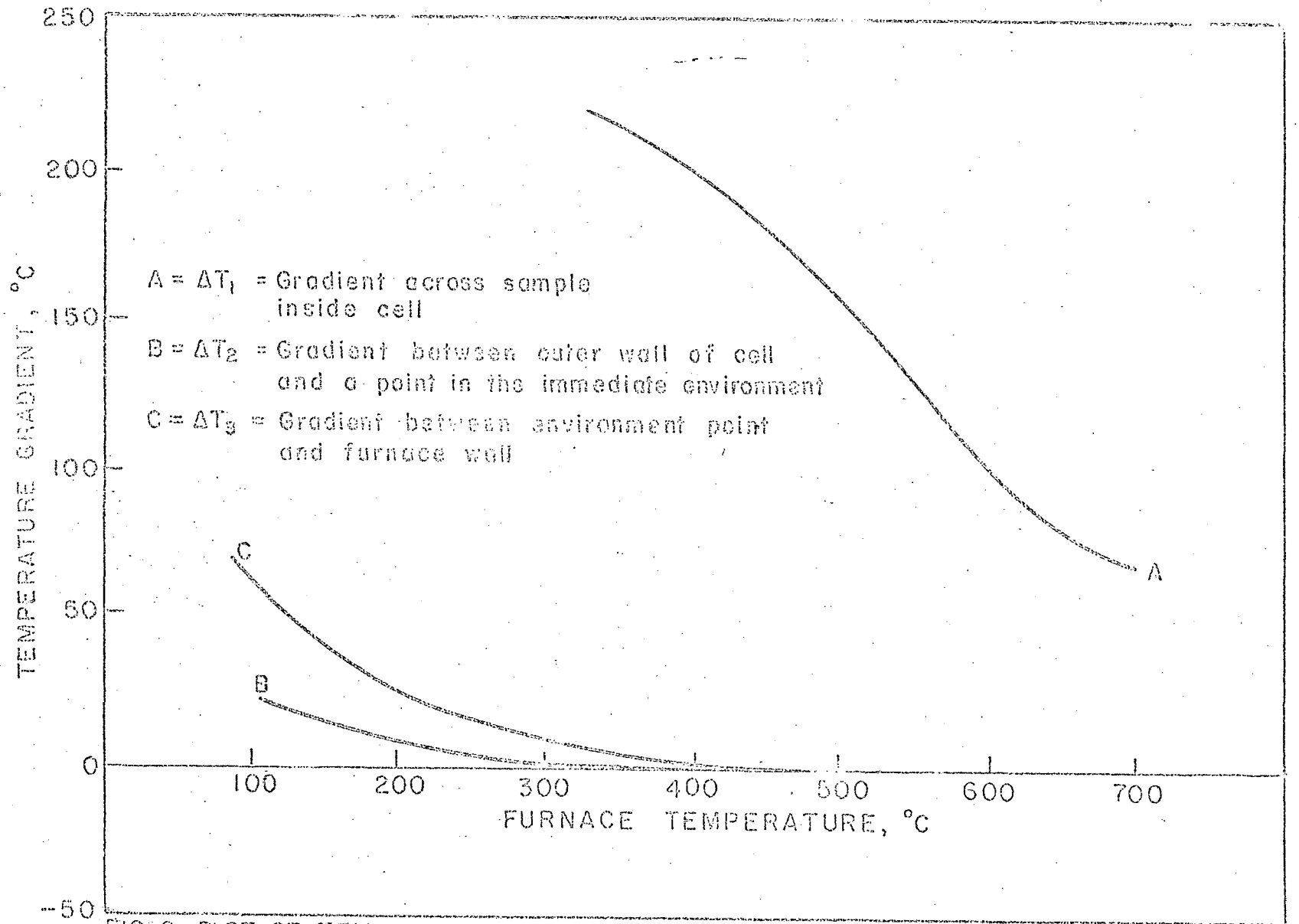

FIG. 9 PLOT OF TEMPERATURE GRADIENT vs. ENVIRONMENTAL FURNACE TEMPERATURE. VACUUM.

in argon,	6×10^{-4} cal/sec/°C/cm	(40°C)
	to 20×10^{-4} cal/sec/°C/cm	(750°C)
in vacuum,	5×10^{-4} cal/sec/°C/cm	(350°C)
	to 15×10^{-4} cal/sec/°C/cm	(750°C) .

The "effective" conductivity of the immediate cell environment (K_3) increased rapidly with temperature in helium (20×10^{-4} cal/sec/°C/cm at 100°C to 200×10^{-4} cal/sec/°C/cm at 550°C). In argon this increase was much less marked (20×10^{-4} at 100°C to 150×10^{-4} cal/sec/°C/cm at 700°C). The effective thermal conductivity of this region is the controlling factor in the temperature gradient value ΔT_2.

Summarizing, helium gives the system with the best response and the lowest and most consistent gradient across the sample. It is, however, less effective than argon in maintaining the $T_3 > T_4$ condition.

VII. USE OF ENVIRONMENTAL INSULATION AROUND THE DIFFERENTIAL THERMAL CALORIMETER CELLS

A. Introduction

The key condition for maintaining the desired heat flow is that $T_3 > T_4$. In the last investigation it was seen that an argon atmosphere was better than the other two in this respect. The superiority of argon was primarily due to its low heat transfer coefficient. It is possible to make the heat conductivity of this section even lower by incorporating a solid insulator around the cell. Such an insulator would eliminate convective and radiative heat transfer in the cell environment and this would stabilize the value of ΔT_3. The problems of the small gradient across the cell and the sensitivity of the empty cell would also be solved, for a helium atmosphere could be used with no detriment to the insulator modus operandi. In consequence of this, the cell complex was again modified.

B. Procedure

Sections of 2500°F insulating brick were carefully cut and drilled to the size required to accommodate the cells in the furnace. The outer diameter of these sections was made to be a snug fit inside the furnace tube. Holes were drilled through the insulating components to carry the thermocouple and powder leads from the cells to the outside circuits. A breakdown of the assembly is shown in Fig. 10. The whole complex was held in the furnace by supporting the bottom of the insulating column.

A series of runs were performed under the same conditions as in part VI; however, the vacuum runs were abandoned as the cell gradient was too large to ever give accurate results. Also, vacuum made the response of the empty cell so slow as to make control impossible.

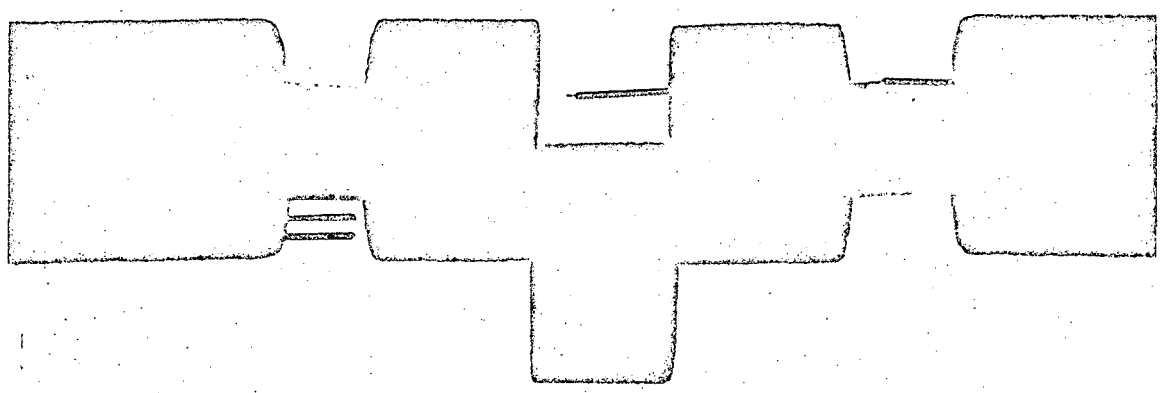

Fig. 10. Cells and insulating brick complex.

Plots of temperature gradients were made as before and these are shown in Figs. 11 and 12.

C. Discussion of Results

The introduction of the insulation around the cells had a marked effect on all the effective conductivity values (see Table III). The conductivity across the cell, K_1, showed very little variation with temperature even at high temperatures in both helium and argon atmospheres. The effective conductivity between the cell wall and its immediate environment was also considerably improved, although in the case of helium it still increased substantially with increasing temperature.

The temperature gradient-vs-temperature plots are observed to more closely approach the ideal parallel horizontal lines discussed in the last section. The gradient across the cells, however, in both cases is much too high for attaining accurate results.

From the magnitude of the gradient across the cell necessary to preserve the $T_3 > T_4$ condition, it can be inferred that the cell insulation needs to be further improved. To do this a value of K_2 close to that of K_1 is required.

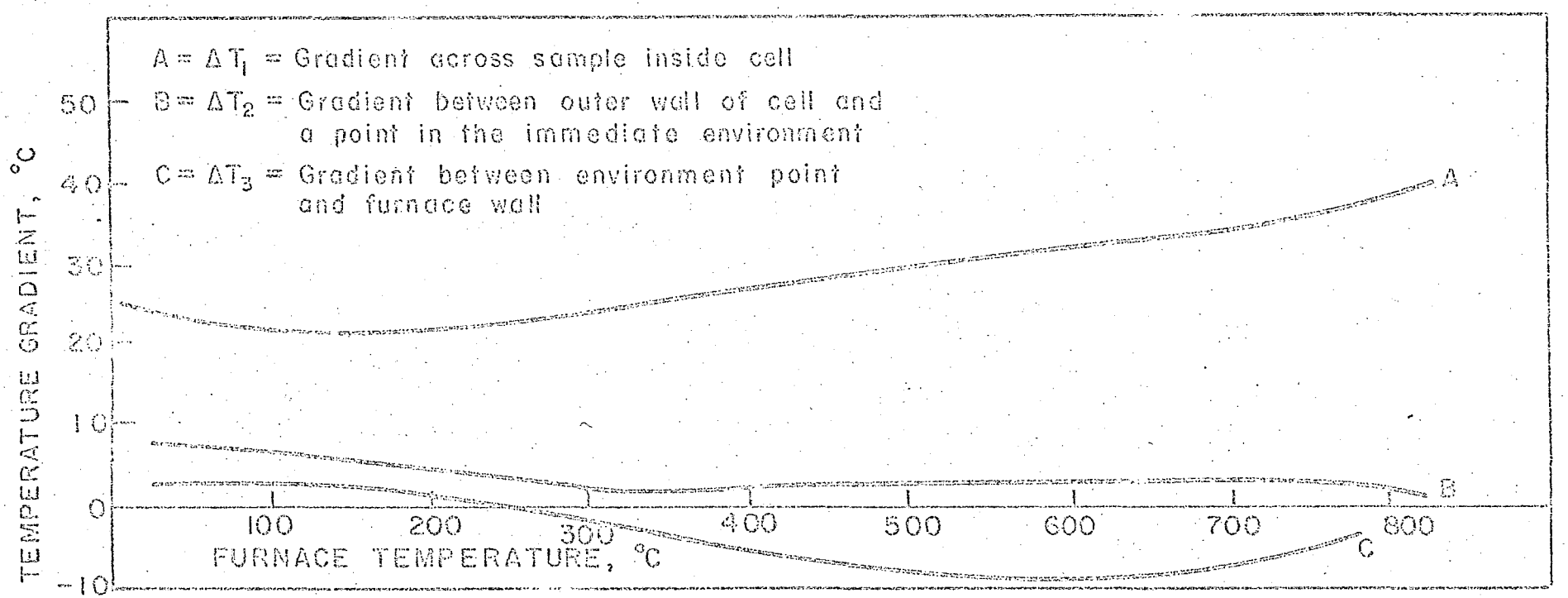

FIG. 11 PLOT OF TEMPERATURE GRADIENT vs. ENVIRONMENTAL FURNACE TEMPERATURE. HELIUM ATMOSPHERE.

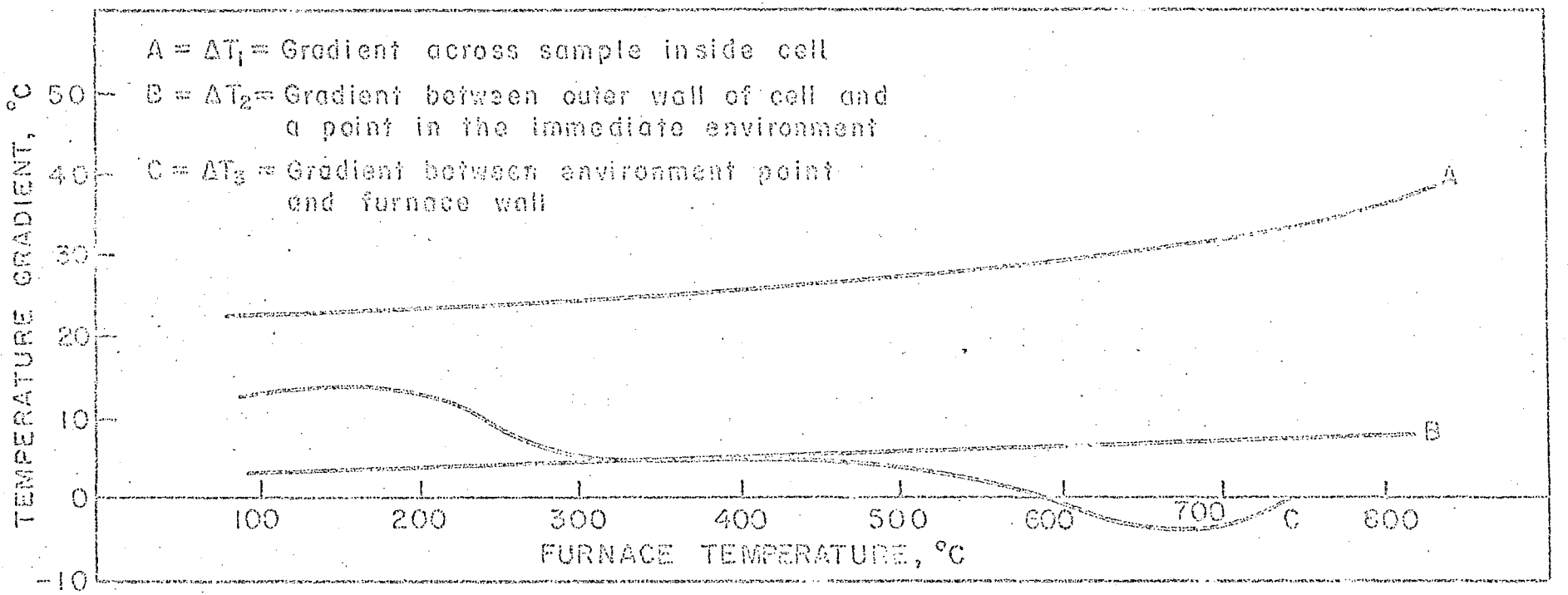

FIG. 12 PLOT OF TEMPERATURE GRADIENT vs. ENVIRONMENTAL FURNACE TEMPERATURE. ARGON ATMOSPHERE.

Table III. Effective thermal conductivities in helium and argon atmospheres.

Furnace Temperature °C	"Effective" conductivity (cal/°C/cm^2/sec) x 10^{-4} Helium atmosphere K_1	K_2	Argon atmosphere K_1	K_2
25	20	40	8	15
100	20	70	8	20
200	20	135	8	30
300	20	195	8	40
400	20	235	8	45
500	20	300	8	50
600	20	600	8	60
700	20	680	8	110

VIII. USE OF POWDER AS ENVIRONMENTAL INSULATION AROUND THE DIFFERENTIAL THERMAL CALORIMETER CELLS

A. Introduction

The only way to achieve the conductivity level for K_2 discussed previously is to have a packed powder around the cell.

B. Procedure

A thin-walled nickel tube, larger in diameter than the cells, was cut into lengths such that the difference in length between it and a cell was twice the difference of their radii. Boron nitride pieces were then cut which when assembled would fix the cell in the center of the nickel tube. In essence a cell-within-a-cell combination was made. The double cell is shown diagrammatically in Fig. 13. The boron nitride pieces were carefully drilled to facilitate the passage of thermocouples and electrical leads to the inner cell. The two complex cells were assembled on the platinum support wire and the top one was completely filled with ball-milled A-14 alumina. The outer parts of the bottom cell were filled with alumina also. The assemblage was then lowered into the furnace with no extra insulation added. The design of the main furnace was also changed for this series of runs. The heavy nickel tube now itself carried an insulated winding of Kanthal A-1. This tube also traversed the whole furnace length with no collars or supports. The axial heat losses from the core were minimized by turning down the ends of the tube and by double-winding the coil at both ends of its travel. In a test run the heat loss from the ends was very small.

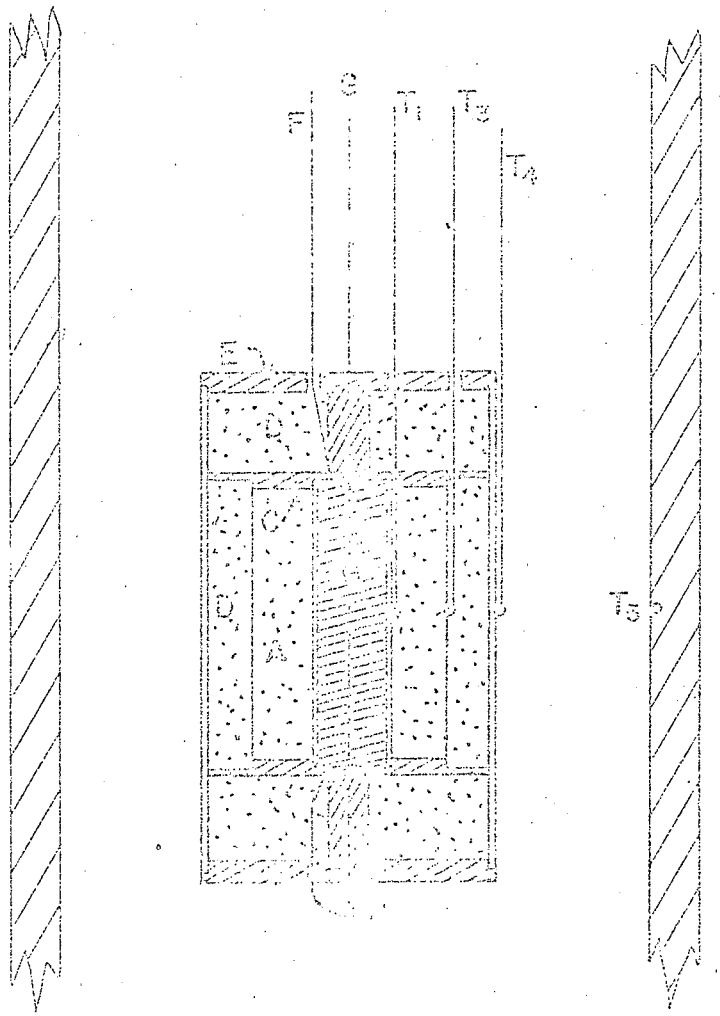

T_1, T_3, T_4 Thermocouple positions

T_5 Thermocouple position in Nickel furnace tube

A Powder sample in Platinum cell

B Cell heater

C Boron Nitride cap and spacer

D Insulating Al_2O_3 powder

E Boron Nitride top cap

F, G Heater leads

H Heater lead wrapped about common support wire G

FIG. 13 DIAGRAM OF DOUBLE-CELL.

Following the same procedure as obtained before, an initial power of 5 W was passed through both cells. The cells were heated in helium and argon atmospheres and the thermal gradients noted. Again, the cell power was increased when conditions required it. The temperature gradients observed were plotted vs temperature and are shown in Figs. 14 and 15.

C. Discussion of Results

In both gases the gradient across the cell and across the immediate cell environment remained very constant with increasing temperature. The size of the sample gradient necessary to maintain correct heat flow conditions was significantly lowered in both cases also. With this cell design, control of the temperature sequence, $T_1 > T_2 > T_3 > T_4$ and especially $T_3 > T_4$, should be possible with no difficulty.

The "effective" conductivity across the sample (K_1) was constant with increase in temperature (K_1 increased at the rate of 0.00007 cal/°C/cm^2/sec/100°C in helium). K_1 in argon was also constant but significantly lower than the value in helium (see Table IV). With the elimination of the difficulty of controlling $T_3 > T_4$, helium atmospheres can be used sans souci. This will increase the accuracy of any calorimetric results also as the sample gradient is small and the system sensitivity maximized.

D. Conclusions

It was observed earlier that for accurate results heat must always flow out of the cell into the environment. This flow of heat depends entirely on the thermal conductivity of the environment. This controls

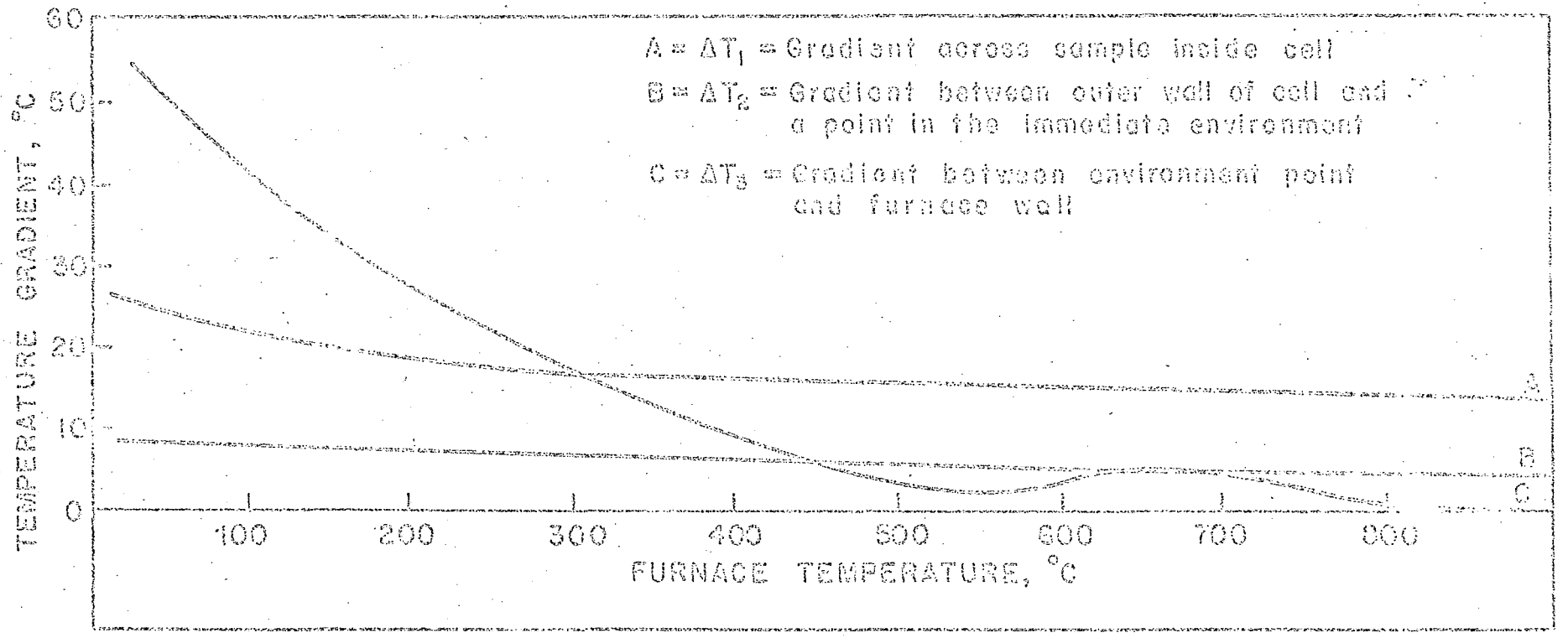

FIG. 14 PLOT OF TEMPERATURE GRADIENT vs. ENVIRONMENTAL FURNACE TEMPERATURE. HELIUM ATMOSPHERE.

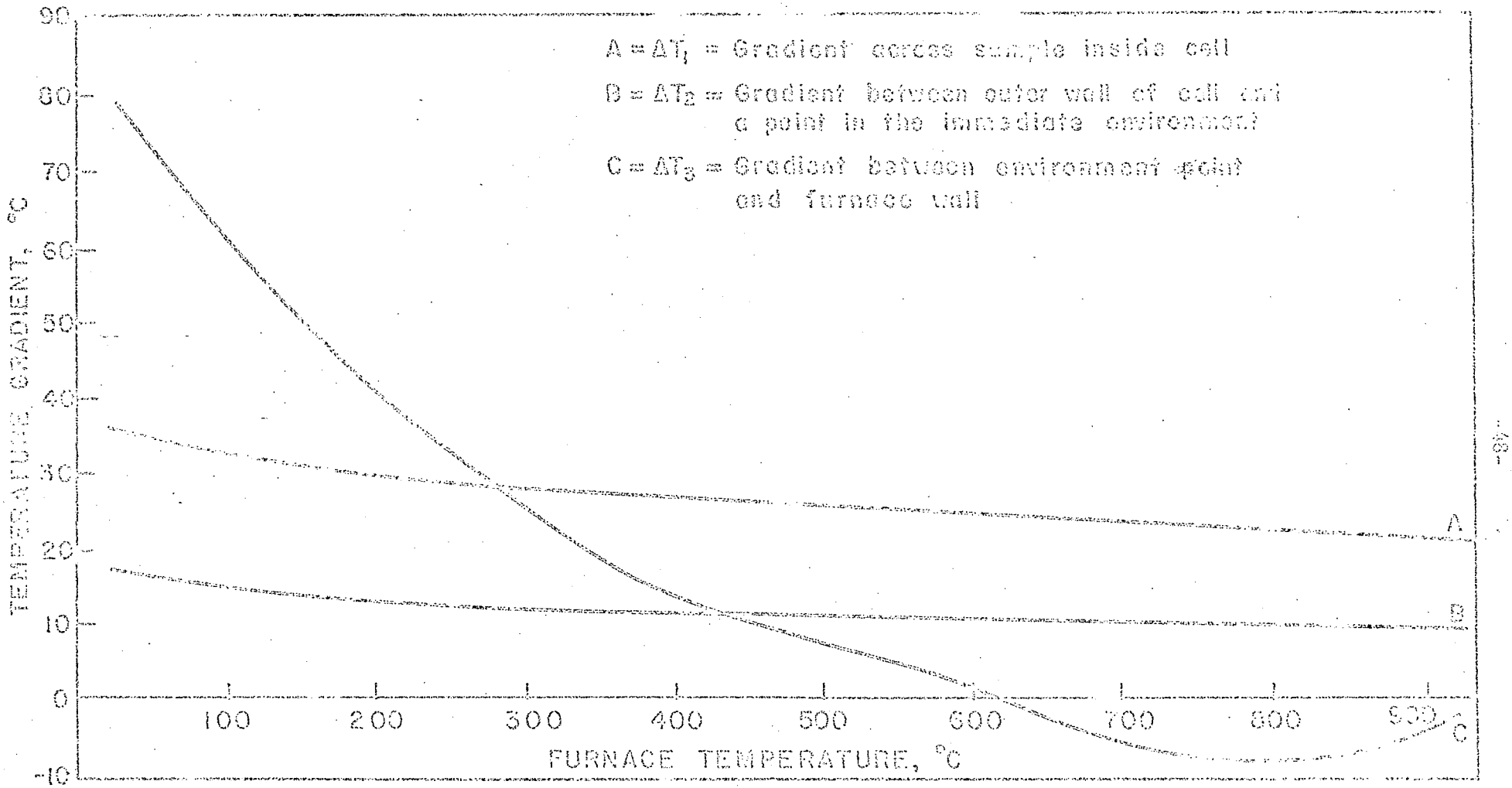

FIG. 15 PLOT OF TEMPERATURE GRADIENT vs. ENVIRONMENTAL FURNACE TEMPERATURE. ARGON ATMOSPHERE.

Table IV. Effective thermal conductivities in helium and argon atmospheres using powder insulation.

Furnace Temperature °C	"Effective" conductivity (cal/°C/cm^2/sec) x 10^{-4} Helium atmosphere K_1	K_2	Argon atmosphere K_1	K_2
25	27	37	16	16
100	27	37	16	17
200	28	36	16	17
300	28	35	16	18
400	29	35	17	18
500	30	37	17	19
600	31	40	18	21
700	32	43	19	24
800	33	43	21	27
900	33	44	23	24

the heat flow <u>into</u> the cell. The value of this thermal conductivity should, therefore, be low and constant with temperature. These conditions have been fulfilled and, therefore, accurate results should be obtainable with cells of this design.

IX. NOTE ON THE POWER REQUIREMENTS OF THE CELLS

Throughout the discussion of the three cell modifications investigated, little has been said concerning the actual power input to the cells. The power was adjusted to ensure heat flow out of the cell at all times. The value of K_2, the immediate cell environment thermal conductivity, dictated the level of power required, i.e., when K_2 increased then more power was needed. Increasing the power in this fashion only serves to decrease the accuracy of any results; hence, ideally the power level should remain constant. In actual fact, the power will never remain constant because the heater resistance increases with temperature. Using the heat flow <u>from</u> the cell as the norm, the power required is plotted in Fig. 16 as a function of temperature. From this it can be seen that the power level maintained in the "double" cell case was the most consistent, and this result further verifies the use of this design for accurate work.

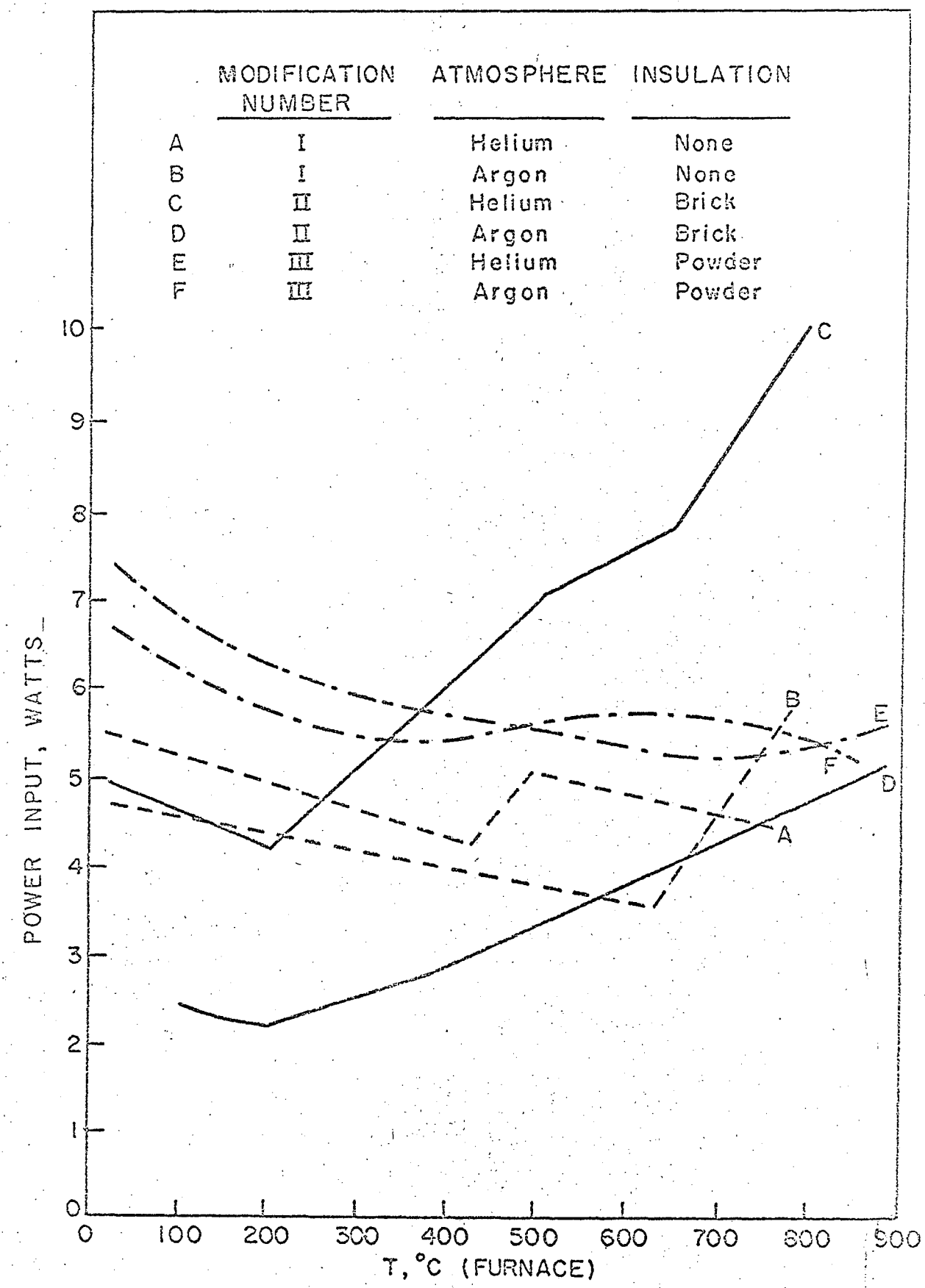

FIG. 16 POWER REQUIRED vs. FURNACE TEMPERATURE.

X. AXIAL HEAT FLOW BETWEEN THE DIFFERENTIAL THERMAL CALORIMETER CELLS

A. Introduction

In the section dealing with the theory of steady-state heat transfer, it was assumed that the axial heat flow in the cell system was negligible. With the double-cell design this approximation is even more valid, for the layers of powder above and below the cell are twice the thickness of the interwall layer. However, axial heat flow can still take place down the platinum support wire. The following investigations were undertaken to estimate the actual errors incurred by this link between the cells.

B. Procedure

The double cells were assembled in exactly the same way as in the previous experiment. They were placed in the furnace and heated to 300° C in helium and then allowed to soak at this temperature. During this time no power was supplied to the cells themselves. On reaching equilibrium, the gradients across the top cell were noted. A power of 5 W was then supplied to both cells and the gradients again noted when equlibrium was once more established. The bottom cell power was then turned off and the effect of this move on the top cell gradients observed. Finally, the top cell was cut off and the bottom cell power turned back on and the gradients in the top cell again noted. This procedure was repeated at 600° C and 900° C and then all the runs were duplicated in argon and in vacuum.

The results are shown diagrammatically in Figs. 17A and B. The heat flow between the cells due to the connecting wire was estimated from the top cell gradients observed in the vacuum run. These results are shown in Table V.

HELIUM

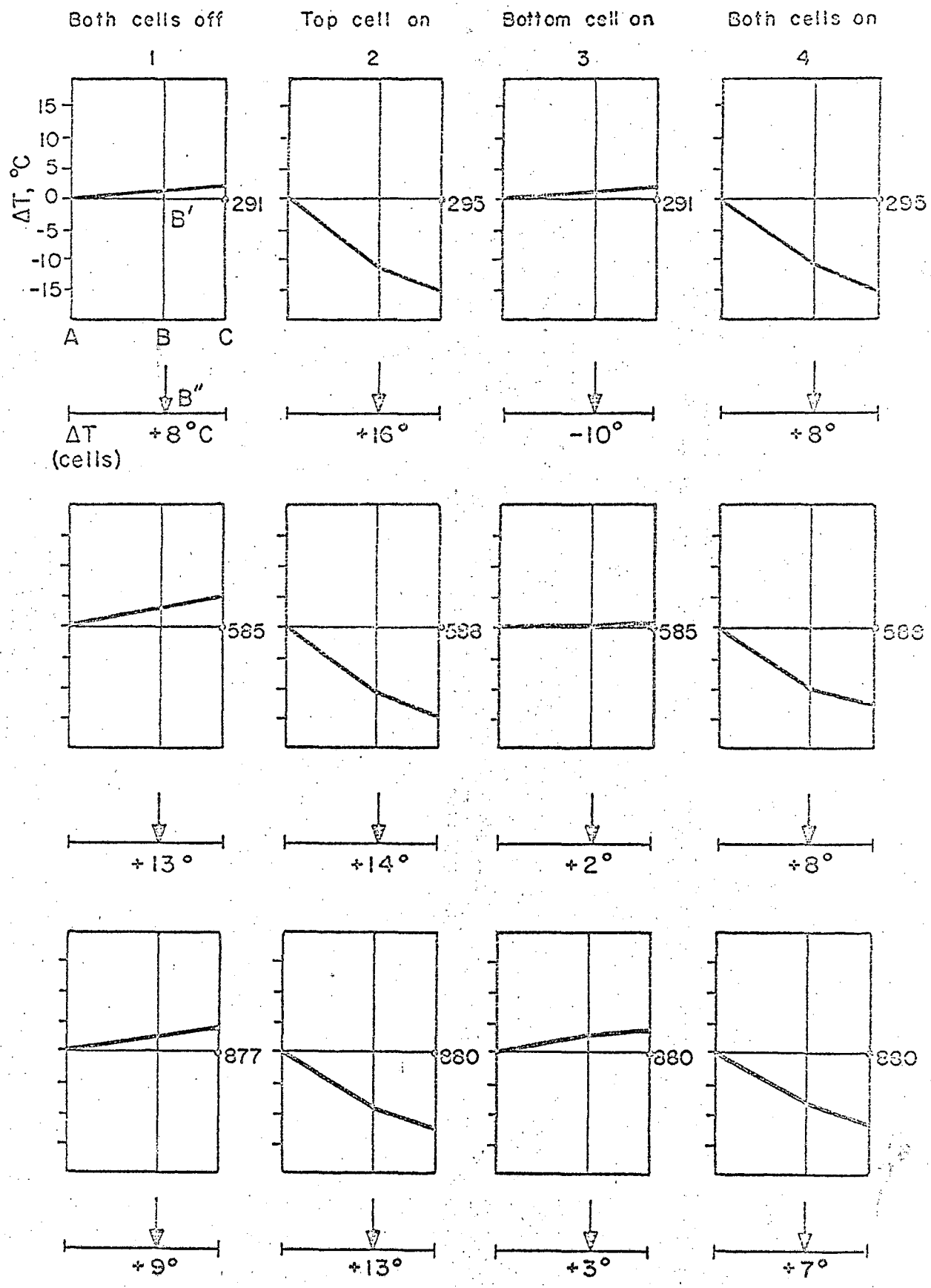

FIG. 17 A.

VACUUM

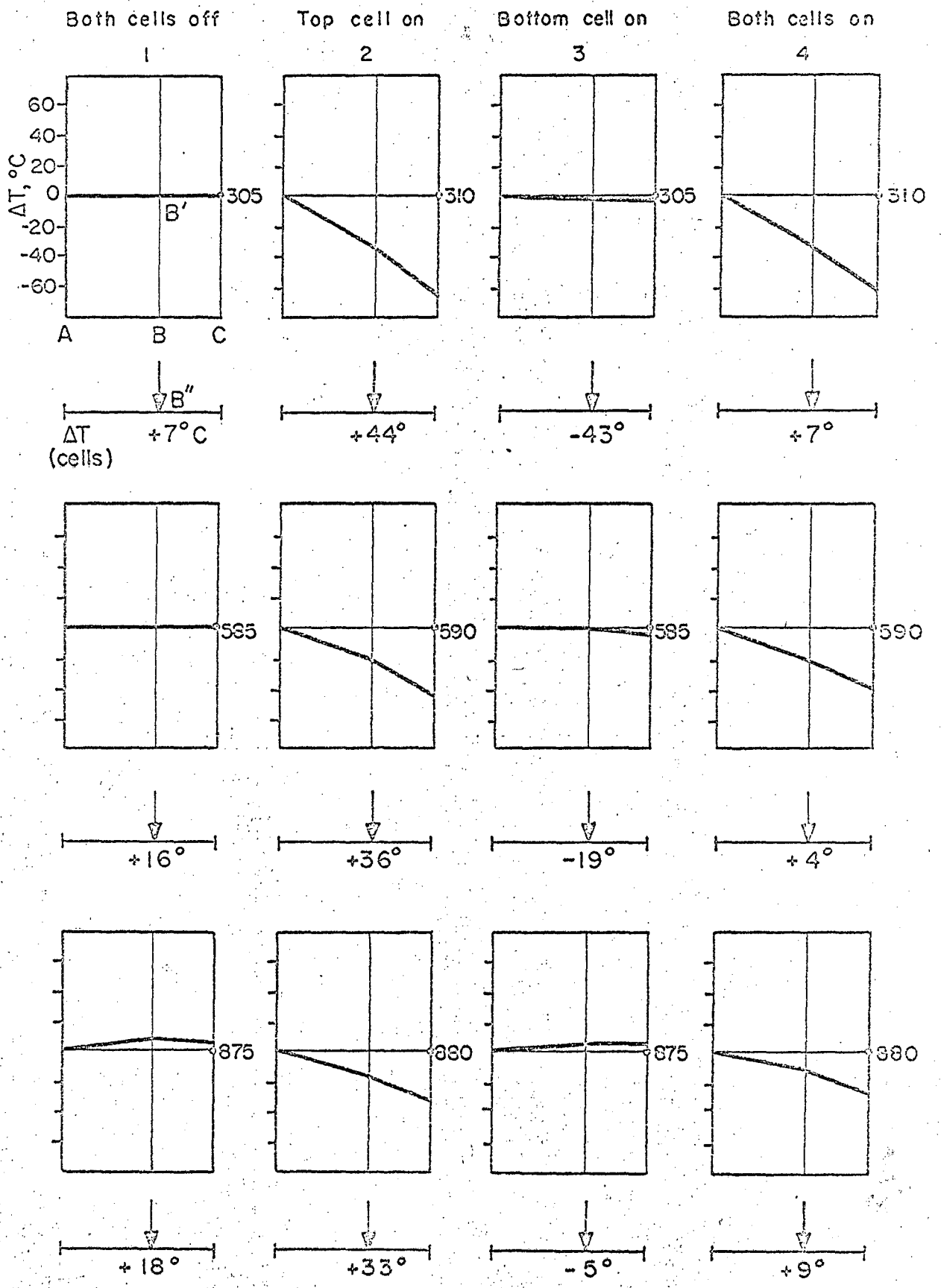

FIG. 17 B.

Table V. Gradients observed in top cell during vacuum run.

Furnace Temperature °C	Gradient Both cells off °C	q_1 cal/sec	Gradient Bottom cell on °C	q_2 cal/sec
300	0	0	+1	0.03 ↑*
600	0	0	0	0
900	-3	0.26 ↓*	-2	0.17 ↓*

*Arrows indicate direction of heat flow.

C. Discussion of Results

In Fig. 17, each little diagram represents a section of the filled cell under different conditions. Line A is the inner cell wall, B the cell outer wall, and C the outer wall of the enclosing cell. The monitor thermocouple is located on C and its reading is given in each case. The gradient is shown plotted vertically about the center line of each diagram. The scale is the same for each case and so is not repeated. Using the inner wall of the cell as a reference, the gradients observed are plotted for each of the conditions stated at the head of columns. Underneath each figure the center line of the bottom cell is shown. The arrow B" indicates a point corresponding to the point B' in the top cell. Underneath the arrow the differential temperature observed between B" and B' is shown. A positive value of this gradient indicates that B' > B".

Thermal linkage between the cell is best demonstrated in vacuum. Considering the case when the bottom cell alone is on (in vacuo), the effects of this cell on the top one can easily be seen. When the bottom cell is 43°C hotter (Fig. 17B, row 1, column 3), it induces a slight + ve gradient in the top cell. As the temperature difference between the cells goes down, this positive gradient gives way to a negative one. The gradient across the top cell when the bottom is hotter by 5°C (row 3, column 3) denotes a supply of heat to the bottom cell by the top one. Utilizing the standard steady-state thermal conduction equation,

$$q = \frac{k 2\pi \ell \, \Delta T}{\ln r_o/r_i} ,$$

where k is the thermal conductivity of packed powder in vacuo, ℓ is the cell length, and r_o and r_i are the cell outer and inner radii. Then q_1, the heat flow in cal/sec, can be obtained. Let q_1 be the heat flow across the top cell when both cells are off and q_2 the same flow when the bottom cell is on. On reaching the center of the cell, the heat will divide (as the platinum wire passes through the cell center). Hence, the quantity q_1 may be written

$$q_1 = p_1 + p_2 , \tag{16}$$

where p_1 and p_2 are the amounts of heat flowing up and down the wire, respectively. Likewise, with q_2

$$q_2 = p_3 + p_4 . \tag{17}$$

Assuming that conditions above the top cell are unchanged by the heating of the bottom cell, then

$$p_2 = p_4$$

and hence

$$q_2 = p_3 + p_2 . \tag{18}$$

Solving simultaneously Eqs. (16) and (18),

$$q_1 - q_2 = p_1 - p_3, \tag{19}$$

where p_1 and p_3 are both heats flowing down the wire from the top cell to the bottom cell.

Now $p_1 \propto \Delta T_1$ and $p_3 \propto \Delta T_2$; therefore,

$$q_1 - q_2 \alpha (\Delta T_1 - \Delta T_2) \tag{20}$$

from

$$q_1 - q_2 = \frac{k 2\pi \ell (\Delta T_1 - \Delta T_2)}{\ln r_o/r_i}$$

where ΔT_1 and ΔT_2 are the gradients between the two cells for the two conditions.

Consider the vacuum investigation at 900° C (Fig. 17B, row 3, column 1). When both cells are off, $\Delta T_{cells} = +18°C = (\Delta T_1)$. When the bottom alone is on, then $\Delta T_{cells} = -5°C = (\Delta T_2)$. Using Eq. (13) the values of q_1 and q_2 can be obtained and then applying Eq. (20): $[(q_1 - q_2) \alpha$ (13° C differential between the cells)]. It was found that a differential temperature between the cells of +13° C at 875° C induced a heat flow of 0.0895 cal/sec from the top cell to the bottom cell. The total power input to each cell was 1.2 cal/sec. Hence, if one cell gets 13° C cooler than the other, 7.5% of the power fed to the hotter cell will go to the cold one.

It has been assumed throughout all the experiments reported that the actual gradient down the furnace was uniform. However, the results in column 1 of Fig. 17B show this not to be so. At 900° C, a natural gradient of 18° C was noted. With such gradients, an error of +7.5% must be involved in any thermal change measured. To eliminate this source of error, the cells should be in an isothermal environment.

XI. DESIGN OF A DIFFERENTIAL THERMAL CALORIMETER CAPABLE OF PRODUCING ACCURATE RESULTS

Following the basic precepts required for accurate work, a double-cell design has been arrived at. Augmenting this, it has also been found that accuracy requires an isothermal cell environment and isolation of the cells one from the other.

The best approach that can be made to isothermal conditions is to surround the cells with a material of high thermal conductivity. Such a material would have to be a metal. One design that would fulfill all these stipulations is a block of metal with two large circular wells drilled side by side in it to accommodate the cells. The cavities would be much deeper and wider than the cells so that powder could be packed around the cells. The cells could be held in position by spiders of a low conductivity material. In this way the double cells would be completely isolated from each other in an isothermal environment.

A. Design Principles

In such a system, heat will flow from a cell both axially and radially. For accurate work, it is essential that the axial heat flow should be very small. Fixing the depth of insulating powder above and beneath the cell at 2 in., it is possible to work out the powder thickness around the cell for a given radial/axial heat-flow ratio.

Let the rate of heat flow, q_1, through the powder radially be 20X that through the powder axially. Let the ΔT across each section be the same. Application of the standard steady-state heat flow equations gives, therefore,

$$q_1 = \frac{k_e 2\pi \ell \Delta T}{\ln r_2/r_1} \quad \text{(radially)}$$

and

$$\frac{q_1}{20} = 2\left[\frac{k_e \pi r_1^2 \Delta T}{\ell'}\right] \text{(axially)} ,$$

where k_e is the effective conductivity, ℓ is the length of cell, r_1 is the radius of cell, r_2 is the radius of outer cell, and ℓ' is the powder thickness beneath the cell. Equating these two and letting $\ell = \ell' = 2$ in. and $r_1 = 1/2$ in. then

$$\ln r_2/r_1 = \ell^2/20r_1^2$$

which gives $r_2 = 1.1$ in.

Thus, assuming a 2 in. thickness of insulating powder above and below the cell, the powder thickness around the cell must be 1.1 in. to ensure that only 1/20 of the total heat from the cell flows axially. The practical heat flow axially will be much less, for the cell has boron nitride ends and platinum walls.

If the cells are to be in the same isothermal environment, the isotherms in the surrounding metal must be equal and circular about each cell. The closest practical approach to this is shown in Fig. 18. The cells are centered at the centers of the two end semicircles. The section is of such a length that each cell has an equal circle of metal around it. The radii of these circles are the same as that of the end semicircles. In this way the mass of metal is kept down to a minimum. The isotherms in such a block will not be circular, but their shape will be identical around each cell. The advantage of this design is that the heating coil can be wound directly on the block periphery

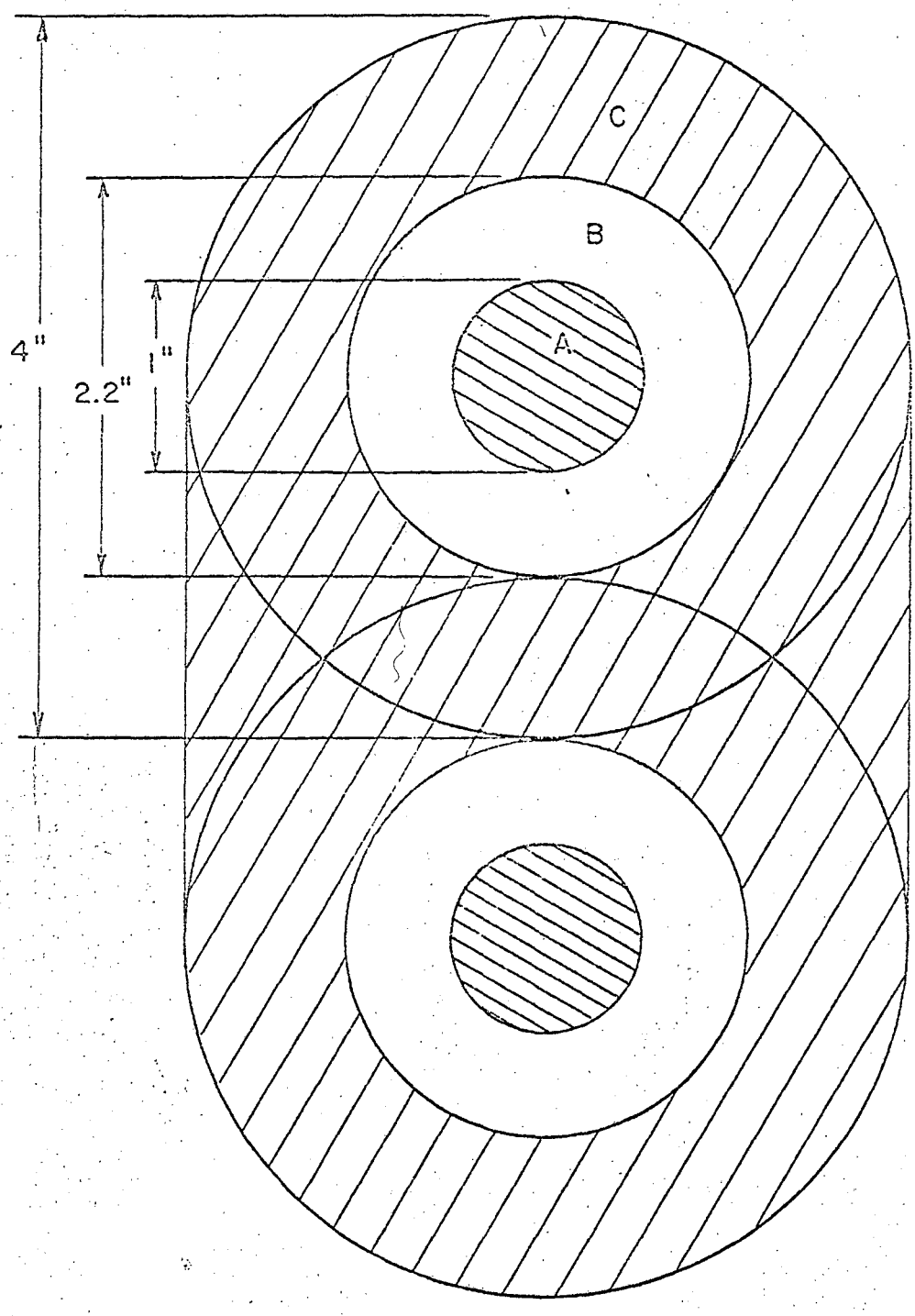

A. Cell
B. Insulating powder
C. Metal

FIG. 18

so eliminating the problem of erratic heat transfer to the block and hence to the cells. A detailed drawing of the cell assembly is shown in Fig. 19.

The filled cell (A) is held in the center of the powder-filled cavity by the two boron nitride spiders (J). The lower spider is supported on a fine ring of metal. Thermocouples C, D, E, and G enter through the base of the metal block and C, D, and E are linked differentially in such a way that E records the actual temperature and C and D the differential gradients from this temperature. G is the differential thermocouple controlling the input of power to the empty cell. The center heaters of the cells have their leads (F) also emerging from the base of the block. Thermocouple H monitors the block temperature and controls the power input to the furnace winding. The empty cell is supplied with dummy leads K to balance the outlets from the full cell. The thermocouples in the cells are situated in the actual walls of the cells so dispensing with the platinum foil. The lid L is centered by means of three pins and the base plate M attached by two countersunk screws. A Kanthal-A former, insulated with porcelain beads, is wound in grooves around the whole block. The whole assembly is grounded through rod O which is welded to the block.

The relevant dimensions arrived at by the heat transfer analysis are also shown in Fig. 19. Figure 18 is an elevation of this figure. One advantage of such a design is the ease of loading and unloading of the sample cell, for none of the electrical leads need ever be touched.

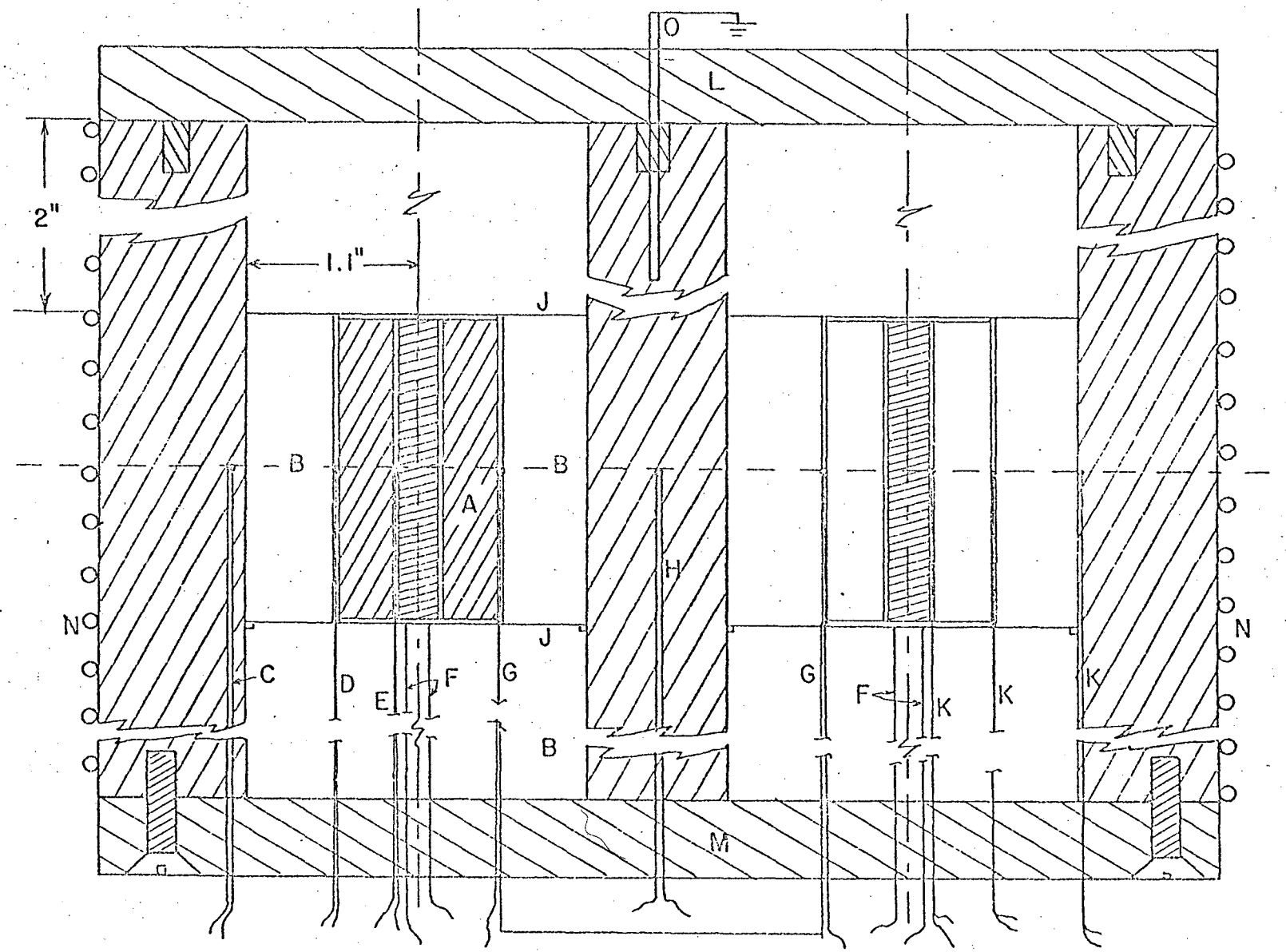

FIG. 19 CUT-AWAY VIEW OF ISOTHERMAL DOUBLE-CELL COMPLEX.

XII. SUMMARY

Following the work of Clareborough and Barner, an attempt has been made to discover the sources of error inherent in these early designs.

The first step in this investigation was to outline the conditions which must be met if the apparatus is to function accurately. It was postulated that

(a) There must be complete symmetry within the system.

(b) The heater in the center of the cell must supply all the the heat required by the sample.

(c) For sensitive control, the response of the active or empty cell must be as quick as possible.

(d) The gradient across the sample must be as low and as constant as possible.

(e) All heat must flow radially from the heater and, therefore, axial heat flow must be minimized.

(f) The cells must be thermally and electrically isolated from one another as far as possible.

The whole assemly was redesigned so that complete symmetry was achieved. The thermal gradients across the whole system were then investigated and it was found that to maintain the heat flow away from the cell, the temperatures across it must follow a definite sequence. The controlling factor in the heat flow was found to be the differential temperature between the cell outer wall and its immediate environment. It was found that the effective thermal conductivity of this section of the system increased rapidly with temperature. Modifications of cell

design were then undertaken in order to control this undesirable increase. It was found that the use of a double cell with insulating powder between the inner and outer walls procured the necessary control. It was demonstrated that the thermal conductivity of a packed powder is very dependent on the gas phase within it. For this reason, the gradient across the sample cell and the sensitivity of the empty cell are both linked with the effective conductivity of the gas in the system. The lowest gradient and the best control were given by a helium atmosphere and so this was adopted.

In the final section of the work, investigations of the axial heat flow from the cells were made. It was found that natural gradients within the cell environment could produce quite marked axial heat transfer. To eliminate this, isothermal conditions around the cells are desirable. A small direct thermal link between the cells was demonstrated, but under isothermal conditions the error incurred by this would be negligible.

Consideration of all the findings led to a design of a calorimeter which would meet all the conditions postulated for accurate results. This design incorporates the cells into a block of metal. Each cell is accommodated in a circular cavity in the block. The intervening space between the cell wall and the cavity sides is filled with a fine powder. The cavities are side by side so isolating the cells from each other. All the thermocouples and electrical leads emerge from the base of the block, facilitating easy emptying and filling the sample cell. By fixing on certain dimensions in the new system, the improved design was worked out in detail.

ACKNOWLEDGMENTS

The author wishes to thank Professor R. M. Fulrath for his help and guidance in conducting this work. Acknowledgment is also extended to D. P. H. Hasselman, R. L. Moon, and R. E. Rose for many helpful suggestions.

This work was done under the auspices of the U. S. Atomic Energy Commission.

REFERENCES

1. J. A. Pask, Differential Thermal Analysis A Tool in Reaction Studies, Pac. Coast Ceram. News, March-April (1953).
2. I. Barshad, Temperature and Heat of Reaction Calibration of the Differential Thermal Analysis Apparatus, Am. Mineralogist 37, 667 (1952).
3. M. Wittels, The Differential Thermal Analyzer as a Micro-Calorimeter, Am. Mineralogist 36, 615 (1951).
4. S. L. Boersma, A Theory of Differential Thermal Analysis and New Methods of Measurement and Interpretation, J. Am. Ceram. Soc. 38, 281 (1955).
5. R. B. Bird, W. E. Stewart, and E. N. Lightfoot, Transport Phenomena (John Wiley and Sons, Inc., New York, 1960), p. 255.
6. A. Euchin, Physik Zeit. 14, 324 (1913).
7. C. M. Clareborough, M. E. Hargrieves, and G. W. West, The Release of Energy during the Annealing of Deformed Metals, Proc. Roy. Soc. (London) A232, 252 (1955).
8. J. O. Barner, Design of a Differential Calorimeter Suitable for Measurement of High Temperature Heats of Solid State Reactions (M.S. Thesis), Lawrence Radiation Laboratory Report UCRL-10631, January 29, 1963 (unpublished).
9. K. K. Kelley, Contribution to Data on Theoretical Metallurgy XIII. High Temperature Heat Content, Heat Capacity, and Entropy Data for the Elements and Inorganic Compounds, U.S. Bur. Mines Bull. 584 (1960).
10. W. H. McAdams, Heat Transmission, Second Edition (McGraw-Hill Book Co., New York, 1942), p. 237.

This report was prepared as an account of Government sponsored work. Neither the United States, nor the Commission, nor any person acting on behalf of the Commission:

A. Makes any warranty or representation, expressed or implied, with respect to the accuracy, completeness, or usefulness of the information contained in this report, or that the use of any information, apparatus, method, or process disclosed in this report may not infringe privately owned rights; or

B. Assumes any liabilities with respect to the use of, or for damages resulting from the use of any information, apparatus, method, or process disclosed in this report.

As used in the above, "person acting on behalf of the Commission" includes any employee or contractor of the Commission, or employee of such contractor, to the extent that such employee or contractor of the Commission, or employee of such contractor prepares, disseminates, or provides access to, any information pursuant to his employment or contract with the Commission, or his employment with such contractor.